

JGR Solid Earth

REVIEW ARTICLE

10.1029/2021JB023141

Special Section:

Understanding and anticipating Induced Seismicity: from mechanics to seismology

Key Points:

- Pore-fluid pressure diffusion remains a basic mechanism for initiating induced seismicity in the vicinity of fluid injection
- Poroelastic stress, Coulomb static stress, and aseismic slip also contribute to triggering seismicity beyond the influence of pressure diffusion
- Research opportunities exist in developing fully coupled models and integrating process-oriented models to study induced seismic hazard

Correspondence to:

S. Ge,
shemin.ge@colorado.edu

Citation:

Ge, S., & Saar, M. O. (2022). Review: Induced seismicity during geoenery development—A hydromechanical perspective. *Journal of Geophysical Research: Solid Earth*, 127, e2021JB023141. <https://doi.org/10.1029/2021JB023141>

Received 2 SEP 2021
Accepted 17 FEB 2022

Author Contributions:

Conceptualization: Shemin Ge, Martin O. Saar

Formal analysis: Shemin Ge, Martin O. Saar

Methodology: Shemin Ge, Martin O. Saar

Resources: Shemin Ge

Writing – original draft: Shemin Ge, Martin O. Saar

Writing – review & editing: Shemin Ge, Martin O. Saar

© 2022 The Authors.

This is an open access article under the terms of the [Creative Commons Attribution-NonCommercial License](https://creativecommons.org/licenses/by-nc/4.0/), which permits use, distribution and reproduction in any medium, provided the original work is properly cited and is not used for commercial purposes.

Review: Induced Seismicity During Geoenery Development—A Hydromechanical Perspective

Shemin Ge¹  and Martin O. Saar^{2,3} 

¹Department of Geological Sciences, University of Colorado Boulder, Boulder, CO, USA, ²Department of Earth Sciences, Geothermal Energy and Geofluids Group, Zurich, Switzerland, ³Department of Earth and Environmental Sciences, University of Minnesota, Minneapolis, MN, USA

Abstract The basic triggering mechanism underlying induced seismicity traces back to the mid-1960s that relied on the process of pore-fluid pressure diffusion. The last decade has experienced a renaissance of induced seismicity research and data proliferation. An unprecedented opportunity is presented to us to synthesize the robust growth in knowledge. The objective of this article is to provide a concise review of the triggering mechanisms of induced earthquakes with a focus on hydro-mechanical processes. Four mechanisms are reviewed: pore-fluid pressure diffusion, poroelastic stress, Coulomb static stress transfer, and aseismic slip. For each, an introduction of the concept is presented, followed by case studies. Diving into these mechanisms sheds light on several outstanding questions. For example, why did some earthquakes occur far from fluid injection or after injection stopped? Our review converges on the following conclusions: (a) Pore-fluid pressure diffusion remains a basic mechanism for initiating inducing seismicity in the near-field. (b) Poroelastic stresses and aseismic slip play an important role in inducing seismicity in regions beyond the influence of pore-fluid pressure diffusion. (c) Coulomb static stress transfer from earlier seismicity is shown to be a viable mechanism for increasing stresses on mainshock faults. (d) Multiple mechanisms have operated concurrently or consecutively at most induced seismicity sites. (e) Carbon dioxide injection is succeeding without inducing earthquakes and much can be learned from its success. Future research opportunities exist in deepening the understanding of physical and chemical processes in the nexus of geoenery development and fluid motion in the Earth's crust.

Plain Language Summary Earthquakes can be triggered by fluids injected into deep underground. Critical knowledge on how they happened has been accumulating since the mid-1960s after a magnitude 5 earthquake shook Denver, CO, USA. The main culprit is the pore-fluid pressure in rocks weakening and reactivating existing faults, which leads to earthquakes. The last decade has experienced a renaissance of fluid triggered seismicity research due to the robust development of oil and gas as well as exploration of geothermal energy. This article reviews four processes that contribute to triggering earthquakes: pore-fluid pressure from injection weakening faults, poroelastic stresses from injection, stresses from earlier earthquakes, and cumulating stresses from aseismic slip. Discussions are presented to address several outstanding questions, for example, why did some earthquakes occur far from fluid injection or after injection? The review leads to following conclusions. (a) Pore-fluid pressure diffusion remains important for initiating earthquakes near injection. (b) Poroelastic stresses and aseismic slip contribute to inducing seismicity far from injection. (c) Stresses from earlier earthquakes can increase stresses on mainshock faults. (d) Multiple mechanisms often operate to induce earthquakes. (e) CO₂ injection is succeeding without inducing earthquakes and lessons can be learned. Future research opportunities exist in understanding induced earthquake hazards.

1. Introduction

Unintended earthquakes from grand-scale human experiments began to unfold as early as late 1800 to early 1900 when felt earthquakes were induced by mining and reservoir impoundment (McGarr et al., 2002). Fluid injection into the deep subsurface, contributing to inducing earthquakes, started from the mid-1960s and accelerated in the late 1990s, particularly from activities related to the exploration and development of oil, natural gas, and geothermal energy (e.g., Ellsworth, 2013; Foulger et al., 2018). Data, emerging from induced earthquakes around the globe, offer an unprecedented opportunity that has not only energized seismologists and geomechanists but also hydrogeologists and geodesists to study induced earthquakes from various perspectives. The last decade has experienced a renaissance regarding induced seismicity studies. Human activities come and go as the energy

industry booms or busts, which makes synthesizing and reviewing the substantially increased knowledge over the last decade concerning induced seismicity particularly opportune. It is in this spirit that this review is conceived.

Before expanding the background further, two frequently referred terms are first defined. *Geoenergy development* in this article refers to activities related to exploration and production of geothermal energy and unconventional oil and gas. These activities include wastewater injection, hydraulic fracturing for enhanced geothermal systems (EGS), hydraulic fracturing in low-permeability formations, such as shale for unconventional oil and natural gas production, fluid extraction, and CO₂ sequestration. We note that case examples from these activities discussed in this article were not meant to cover the major cases in their respective fields, geothermal or oil and gas. Rather, they were selected for their relevance to discussing induced seismicity mechanisms. *Induced seismicity* and triggered seismicity have been used to distinguish earthquakes that release strains through fault failure driven by anthropogenic activities and earthquakes that release tectonic strains naturally (e.g., McGarr et al., 2002). In some cases, induced earthquakes can trigger subsequent seismicity (e.g., Ellsworth et al., 2019). In this article, the term induced seismicity is adopted for all earthquakes that could be attributed to, or have been proposed to have occurred as a result of, anthropogenic activities related to geoenergy development. Induced versus triggered will not be distinguished hereafter.

1.1. Fluid Injection Related to Geoenergy Development

Among the reported cases of fluid injection induced seismicity ~34% arise from three types of geoenergy development activities, namely wastewater injection, hydraulic fracturing of unconventional shale reservoirs for oil and gas production, and hydraulic stimulation (fracturing and/or shearing) to generate EGS (Amann et al., 2018; Gischig et al., 2020; Wilson et al., 2017). The remaining 66% is primarily from mining and surface reservoir impoundment. A brief description of each of these operations is presented below.

Wastewater generation over the past decade accompanied the robust growth of unconventional hydrocarbon production from low permeability formations. The main source of the wastewater is produced water, that is, brought to the land surface during the production of oil and natural gas. Such wastewater is typically saline to highly saline with a total dissolved solid concentration greater than 10,000 mg/L. Most produced water constitutes pore water or groundwater naturally occurring in rock formations and previously injected hydraulic stimulation fluids. According to 2012 data, it is estimated that 21.2 billion barrels (3.4 billion m³) of wastewater was produced each year from ~1 million oil and gas producing wells in the United States (GWPC, 2019). Deep well injection is one major means for wastewater disposal. For four states in the United States, Oklahoma, Arkansas, Colorado, and New Mexico, where more than 15 yr of injection data between 1994 and 2014 are readily accessible, Weingarten et al. (2015) estimated that the mean fluid injection rate is ~13,000 bbl/month/well (25,000 m³/yr/well) for ~6,500 wells. Approximately 180,000 disposal wells existed in the east-central USA as of December 2014%, and 2,085% of them were in the states of Texas, California, Oklahoma, and Kansas (Weingarten et al., 2015). Reported studies on wastewater injection induced seismicity, however, have primarily come from North America as we cite throughout this article and limited reports from elsewhere, for example, Colombia (Molina et al., 2020) and China (Lei et al., 2013). Studies have linked the sharp increase in induced seismicity in the east-central USA to shale gas development and wastewater disposal (e.g., Ellsworth, 2013).

Hydraulic stimulation comprises hydraulic fracturing and hydraulic shearing, which is referred as fracking thereafter in the paper for brevity. Fracking was developed in the 1940s for enhancing rock permeability to increase production of oil and gas by creating fractures with fluids that are under high pressure (Solberg et al., 1977). The fractures can be created by tensile failure with fractures being oriented approximately perpendicular to the least principal stress (Hubbert & Willis, 1957). In contrast, hydraulic shearing refers to a process whereby existing fractures are reactivated (Paulding, 1967). Once fractures have been reactivated, that is, sheared, the fracture walls no longer fit together perfectly but rest on asperities that keep them largely apart resulting in enhanced permeability. Often proppants are used to provide additional support to the fracture, propping it apart. Both tensile and shear failures have been demonstrated in laboratory tests under varying background stress and pore-fluid pressure conditions (Lockner & Byerlee, 1977; Solberg et al., 1977).

Hydraulic stimulation to generate EGS was first thought to mainly involve hydraulic fracturing but gradually the approach shifted more toward hydraulic shearing. The technique involves injecting fluid under pressure into hot

crystalline rocks to enhance geothermal fluid circulation. Field-scale EGS research began in the 1970s. Since then it has been attempted to generate large surface areas that promote heat exchange in the subsurface while keeping hydraulic fracturing- or shearing-induced seismicity to a minimum (Amann et al., 2018; Gischig et al., 2020). We note that Riffault et al. (2018) called hydraulic shearing in EGS into question as they observed that the volume of permeability enhancement is much smaller than that of active seismicity. Many earlier EGS development attempts were discontinued before they matured to operational levels for reasons other than induced seismicity (Evans et al., 2012). However, induced seismicity was the main reason for shutting down EGS explorations in Basel, Switzerland (e.g., Deichmann & Giardini, 2009) and Pohang, Korea (Ellsworth et al., 2019), or for affecting developments at Soultz-sous-Forêts in France (e.g., Charléty et al., 2007; Majer et al., 2007) and Berlín in El Salvador (Bommer et al., 2006). Currently, several EGS research sites are being planned or operated worldwide, with a focus on zonal isolation of injection wells to hydraulically stimulate small rock volumes at a time, inducing small (<3 M) earthquakes, whose fracture zones are later connected by through-going wells (Breede et al., 2013).

Fracking for enhancing unconventional oil and gas production involves injecting water mixed with other materials into low-permeability shale formations to create fractures to promote flow of oil and natural gas (Clark, 1949). Until recent years, shale gas fracking has not been considered the main culprit for the resurgence of induced seismicity, despite public misconceptions that equated fracking with earthquakes. Felt or damaging seismicity induced by fracking in shales is uncommon, but there have been several reported cases, where earthquakes were felt or caused damages. Schultz et al. (2020) reviewed fracking induced seismicity cases and reported 12 cases around the world with a magnitude range from M_L 3.0 to M_L 5.7 in 2010–2019.

1.2. Motivation

Induced seismicity related to geoenergy surged in the last decade in the US and around the world. Wastewater injections have induced earthquakes as large as M_w 5.8 (Barbour et al., 2017; Chen et al., 2017) and larger than expected earthquakes from fracking have been increasingly reported (e.g., Ellsworth et al., 2019; Schultz et al., 2020). There are several relevant reviews that offer valuable insights into induced seismicity from various perspectives, and a common theme that emerges from these reviews is the recognition that challenges remain in understanding induced seismicity triggering mechanisms, which motivated this study.

For a comprehensive inventory of human-induced seismicity, Foulger et al. (2018) is an excellent resource, along with a website cataloging cases worldwide (Induced seismicity, 2021). While no exhaustive coverage of existing literature and reviews is intended here, we provide a brief discussion of several relevant reviews in the following.

Nicholson and Wesson (1992) surveyed 40–50 induced seismicity cases in North America, where fluids were either injected or withdrawn from different industrial operations. The review correlated some seismicity cases to background stress conditions, some to high fluid injection pressures, and some to large fluid injection volumes. It recognized that an improved understanding of the pore-fluid pressure and localized stress conditions is needed to explain the complex occurrences of the earthquakes. The discussion of induced seismicity mechanisms is limited in this paper.

Aimed at understanding seismicity during hydrocarbon production, Suckale (2009) compiled over 70 induced seismicity cases where subsurface fluid injections or withdrawals were tied to specific activities, such as secondary recovery or hydraulic fracturing. This review also provided analytical models to assess changes in stress or pore-fluid pressure, following subsurface fluid injection or withdrawal. However, the article also acknowledged hindrances in applying these models due to a lack of fluid production data, that is, difficulties in quantifying the relative significance of these stresses relative to tectonic stresses. Induced seismicity mechanisms were not a focus of this review.

A review by Keranen and Weingarten (2018) placed a strong emphasis on the influence of geology on seismicity triggering processes, such as faults and rock property heterogeneity on pore-fluid pressure diffusion. They also discussed future challenges in needing greater data accessibility, discriminating tectonic versus induced earthquakes, and detecting seismicity at the nucleation stage to better understand triggering mechanisms.

Grigoli et al. (2017) offered a European perspective on monitoring and management of induced seismicity with a technical focus on challenges, that is, on monitoring and discriminating natural versus induced seismicity. They

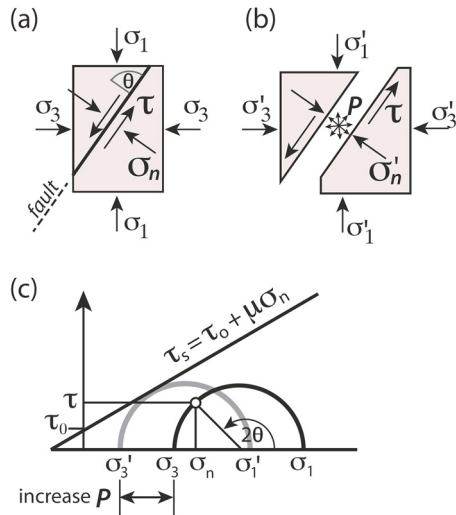


Figure 1. (After Saar & Manga, 2003). Relationship between pore-fluid pressure and stresses on a fault: (a) without pore-fluid pressure change (i.e., $P = 0$), the effective normal stress equals the total normal stress. (b) With a pore-fluid pressure change (i.e., $P > 0$), the effective normal stress is reduced. (c) Mohr circles without (black) and with (gray) pore-fluid pressure changes. The Mohr-Coulomb failure envelope is the diagonal line, where τ_0 and τ_s are cohesion and shear strength, respectively, of the fault, and μ is the friction coefficient.

potential of induced seismicity and called for further research to develop hazard forecast models and mitigation strategies.

1.3. Objectives

Recognition of the basic triggering mechanisms underlying induced seismicity traces back to the mid-1960s when a series of earthquakes shook the tectonically quiescent Denver area, CO USA (Healy et al., 1968; Hsieh & Bredehoeft, 1981). A robust growth in research and new data on this topic proliferated over the past decade as evidenced by the body of work discussed in the above-mentioned reviews and cited in this study. It is worth noting that research on induced seismicity due to the water loading of large hydroelectric reservoirs also experienced a growth since the 1960s (e.g., Ge et al., 2009; Gough & Gough, 1970; Gupta, 2002; Gupta & Chadha, 1995; Talwani, 1997). The objective of this article is to review induced seismicity related to geoenery development with a focus on the physics of triggering mechanisms. Mechanisms in this article refer to mechanical processes that contribute to Coulomb stress changes on faults that lead to triggering seismicity. The review is intended to be accessible to graduate students and researchers at varying stages.

2. Triggering Conditions of Induced Seismicity

2.1. Mohr-Coulomb Friction Theory

The Mohr-Coulomb frictional theory is the foundation to mechanics of fault slip, thus, we first provide a brief summary of it here. Traction is a more precise term for describing forces on a plane, while stress is defined as force over a point. In this article, we use stress also for traction on fault planes, partially because of its wide usage in the induced seismicity literature. In a given stress field, the shear stress (τ) and normal stress (σ_n) on an arbitrarily oriented fault plane can be determined by the three principal stresses and the normal vector of the fault plane (Jaeger et al., 2007, Equations 2.120 and 2.121). Here we illustrate the concept in a simplified two-dimensional setting (Figure 1a) with the assumption that the minimum and maximum principal stresses act perpendicularly to the fault strike. Thus, the intermediate stress (σ_2) drops out of the equations for shear and normal stresses. Then,

offer valuable insights for establishing management guidelines and decision protocols for safer fluid injection operations. This study highlighted pore-fluid pressure diffusion underlying four induced seismicity mechanisms.

Zang et al. (2014) provided an in-depth analysis of induced seismicity in geothermal reservoirs during the different phases of EGS development in various tectonic settings. Specific guidance on monitoring and data analysis were derived for different phases during EGS development and operations. The review also calls for a better understanding of seismicity generation processes, with a particular goal being reducing the probability of inducing large-magnitude events.

Bringing fracking-induced seismicity to the forefront, Schultz et al. (2020) reviewed a dozen cases with earthquake magnitudes from 2.7 to 5.7 and synthesized the commonalities in seismicity origin and styles as well as how seismicity occurrences relate to specific hydraulic stimulation operations. A discussion of possible earthquake triggering mechanisms around fracking sites is also presented.

Recognizing the hazard from fracking induced seismicity, Atkinson et al. (2020) reviewed the current understanding on and research needs for several issues associated with the generation, damage potential, and prediction of fracking induced seismicity. They identified the geomechanical conditions for triggering, pre-existing fault conditions, and fault connection to the stress perturbation. They suggested that it is necessary to better understand how tectonic environments, such as the regional state of stress and fracture networks, affect inducing seismicity. They also highlighted the damage

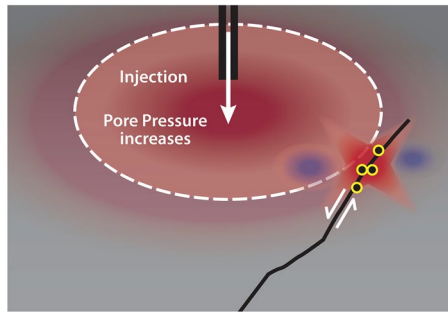


Figure 2. (After Brown & Ge, 2018b). The classic pore-fluid pressure diffusion mechanism for inducing seismicity. Injection causes an increase in pore-fluid pressure (red cloud). When the pressure front (white dashed oval) reaches a critically stressed fault, it reduces the effective normal stress of the fault, which can trigger seismicity.

the shear and normal stresses can be computed by the following equations (e.g., King et al., 1994, Mandl, 1988, p. 235):

$$\tau = \frac{1}{2}(\sigma_1 - \sigma_3) \sin 2\theta, \quad (1)$$

$$\sigma_n = \frac{1}{2}(\sigma_1 + \sigma_3) - \frac{1}{2}(\sigma_1 - \sigma_3) \cos 2\theta, \quad (2)$$

where σ_1 and σ_3 are the maximum and minimum principal stress components. θ is the angle of the fault inclination to σ_1 axis.

Terzaghi (1936) incorporated the effects of pore-fluid pressure (P) on stress and introduced the effective stress concept. The effective normal stress (σ'_n) on the fault is defined as (Figure 1b)

$$\sigma'_n = \sigma_n - P, \quad (3)$$

The Coulomb stress (σ_{cs}) on a fault has been used as a criterion for fault failure. It is defined by (e.g., King et al., 1994):

$$\sigma_{cs} = \tau - \mu(\sigma_n - P), \quad (4)$$

where μ is the friction coefficient of the fault. σ_n is positive for compression.

The Coulomb criterion states that when the Coulomb stress on the fault exceeds a specific value, for example, the shear strength of the fault, failure occurs and the fault slips. Any perturbation, natural or anthropogenic, to the stress field could lead to changes to the Coulomb stresses on faults. For example, a pore-fluid pressure increase will lead to an increase in Coulomb stress. Figure 1c shows how the principal stress components are affected by pore-fluid pressure, an increasing P moves the Mohr circle (black) to the left (gray) and closer to the Mohr-Coulomb failure envelope (diagonal line).

Each of the mechanisms we discuss in the following represents one way to perturb the state of effective stress by changing the shear and normal stresses or the pore-fluid pressure or both on a given fault plane. Such perturbations then resolve the shear stress on a fault plane of interest to overcome the frictional strength of the plane, which leads to the Coulomb stress, defined in Equation 4, be greater than zero. Thus, these mechanisms point to the triggering conditions characterized by changes in the Coulomb stress on faults.

Four mechanisms that have been suggested in the literature are reviewed in this Section. For each, a brief introduction of the basic concept of the mechanism is presented first, which is followed by case examples that are relevant to the corresponding mechanism.

2.2. Pore-Fluid Pressure Diffusion

The classic mechanism of fluid induced seismicity is pore-fluid pressure diffusion. As illustrated in Figure 2, when a fluid is injected into the subsurface, the pore-fluid pressure diffuses away from the fluid injection location, which increases the pore-fluid pressure and reduces the effective stresses in the regions reached by the fluid pressure diffusion. When the elevated pore-fluid pressure encounters faults that are critically stressed, the reduction in effective normal stresses on the faults causes the Coulomb stress acting on the fault to increase and potentially exceed the fault's shear strength, inducing fault slip, triggering seismicity (Figure 1). Critically stressed can be quantified as when the shear stress on a fault approaches the fault's frictional strength. Sequences of earthquakes and larger-magnitude events can subsequently follow. Background stresses and existing critically stressed faults are necessary conditions, pore-fluid pressure diffusion serves as the trigger (Brown & Ge, 2018a; Saar & Manga, 2003). The concept of pore-pressure diffusion triggering seismicity was also applied to infer hydraulic diffusivity by Shapiro et al. (1997).

There are abundant cases, where the classic pore-fluid pressure diffusion mechanism fails to explain observed seismicity that occurred at places, where pore-fluid pressure increases were too small, or at locations beyond the

influence of pore-fluid pressure diffusion, or at delayed times that are inconsistent with reasonable diffusion time scales. For example, it has been reported that the largest seismic events occurred during the post-injection period at some EGS sites (e.g., Charl  ty et al., 2007; H  ring et al., 2008) and numerous wastewater injection sites (e.g., Goebel et al., 2017; Hsieh & Bredehoeft, 1981; Keranen et al., 2013; Ogwari et al., 2018). Other mechanisms need to be evoked for these cases and will be discussed in Sections 2.3–2.5. In the following, we first offer a synopsis of pore-fluid pressure diffusion mechanism and then review the role of other mechanisms, including poroelasticity, Coulomb static stress transfer, and aseismic creep.

2.2.1. Fundamentals

Pore-fluid pressure diffusion, leading to a reduction in effective stresses on faults, has long been a classic, recognized mechanism for inducing seismicity. Under natural equilibrium conditions, the pore-fluid pressure in rocks increases approximately linearly with depth, that is, following hydrostatic conditions. Inevitably, over- and under-pressures exist, deviating from hydrostatic conditions spatially, due to natural heterogeneity of hydrogeologic properties, and temporally, due to past and on-going geologic processes. Human activities can perturb the natural pore-fluid pressure field as well, and the injection of fluid into rock formations is one such human perturbation. The fundamental physics of pore-fluid pressure diffusion is based on the fluid mass conservation principle and Darcy's Law for rocks with incompressible solid grains. It is mathematically described by a diffusion equation (e.g., Ingebritsen & Sanford, 1999)

$$\nabla \cdot [K(\nabla P)] = S_s \frac{\partial P}{\partial t}, \quad K = \frac{k\rho g}{\gamma}, \quad S_s = \rho g(\alpha + n\beta), \quad (5)$$

where P is pore-fluid pressure ($\text{ML}^{-1} \text{t}^{-2}$), K is hydraulic conductivity, k is permeability (L^2), ρ is fluid density (ML^{-3}), g is gravitational acceleration ($\text{L} \text{t}^{-2}$), γ is dynamic fluid viscosity ($\text{ML}^{-1} \text{t}^{-1}$), S_s is specific storage (L^{-1}), and t is time (t), α is the rock bulk compressibility ($\text{Lt}^2 \text{M}^{-1}$), n is porosity (1) and β is fluid compressibility ($\text{Lt}^2 \text{M}^{-1}$). The specific storage S_s represents the change in fluid volume in a unit volume of rock under a unit change in hydraulic head (Freeze & Cherry, 1979). A change in hydraulic head equals a change in pressure head ($\frac{P}{\rho g}$). Equation 5 can be solved for the pore-fluid pressure distribution in time and space employing analytical or numerical methods.

The most relevant formula to fluid-injection perturbed pore-fluid pressure field is the Theis analytical solution from the field of well hydraulics (Theis, 1935). Theis was helped by his colleague C. I. Lubin of the University of Cincinnati and took advantage of the similarity between pore-fluid pressure diffusion and heat conduction by adopting the solution from the heat conduction literature (Carslaw, 1921). It is important to note that the following specific conditions are required for the analytical solution to be applicable. The 2D aquifer domain is laterally infinite and radially symmetric around a line source, the domain is confined on the top and at the bottom by impermeable boundaries, the density and viscosity of the fluid remain constant, and the domain is homogeneous and isotropic. Figure 3 shows the physical setup of the Theis solution. Assuming that the initial pore-fluid pressure field perturbation is zero and that the line source is located at the origin of the radial coordinate system, the analytical solution for diffusion-based pore-fluid pressure changes is given by Theis (1935) as

$$P(r, t) = \frac{Q}{4\pi \left(\frac{k\rho g}{\gamma}\right) b} \int_u^\infty \frac{e^{-u}}{u} du, \quad u = \frac{r^2}{4Dt}, \quad D = \frac{k\rho g}{\gamma S_s}, \quad (6)$$

where Q is the fluid source or sink at $r = 0$ ($\text{L}^3 \text{t}^{-1}$), b is the formation thickness (L), r is the radial coordinate (L), and D is the hydraulic diffusivity ($\text{L}^2 \text{t}^{-1}$).

The analytical solution Equation 6 provides the pore-fluid pressure change as a function of time and radial distance away from the line source, given hydrogeologic properties, under the specified fluid injection or production rate. The solution is applicable to homogenous domains with isotropic permeabilities but can be computed semi-analytically and numerically to take into consideration heterogeneity and permeability anisotropy, for example, due to rock layers (e.g., Wang & K  mpel, 2003). Numerical approaches also enable the computation of pore-fluid pressure variations in irregular and multi-dimensional study domains. Several numerical simulators have

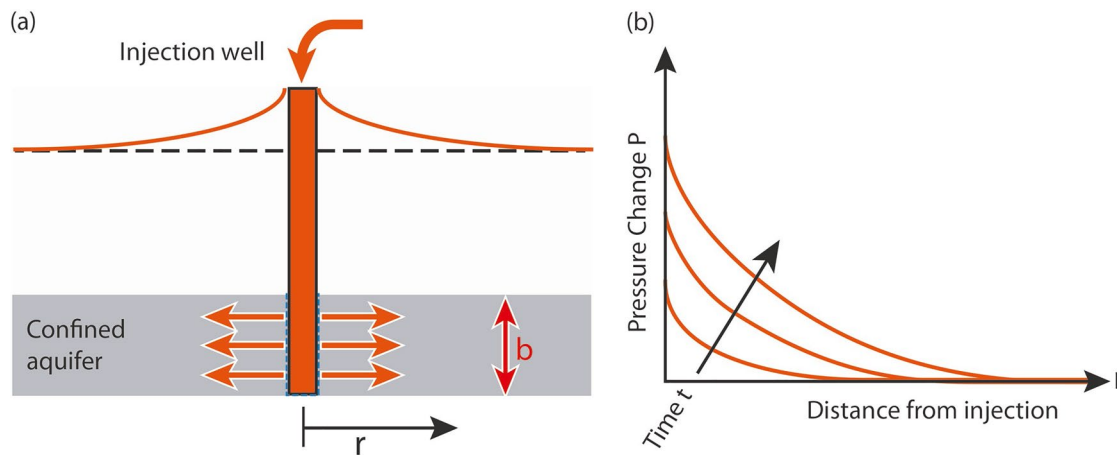


Figure 3. (a) Vertical cross section of the physical system setup for the Theis analytical solution. (b) Conceptual analytical solution (Equation 6) for pressure change with distance and time.

been used to model pore-fluid pressure diffusion inducing seismicity, including the finite difference simulator MODFLOW (Harbaugh et al., 2000) and the multi-physics simulator COMSOL (2018) among others.

There are other analytical solutions to pore-pressure diffusion that are relevant to fluid injection induced seismicity. For example, a point instantaneous mass source Q_0 (L^3) injecting to a large medium at $t = 0$, the pressure change in a spherical coordinate system with the source at $r = 0$ takes the following form (Carslaw & Jaeger, 1959; Rudnicki, 1986, Equation 16):

$$P(r, t) = \frac{Q_0}{(4\pi Dt)^{\frac{3}{2}}} e^{-u} \quad (7)$$

Another example is fluid injection into fractured rocks. Moench (1984) provides an excellent review on dual porosity models for fluid flow in fractured rocks. Briefly, the idea is to consider a fractured porous medium as two interacting and overlapping continua, one being the low-permeability high-storage rock matrix and one being high-permeability low-storage fractures, a dual porosity concept proposed by Barenblatt et al. (1960). While permeability distinction between rock matrix and fractures is apparent, the storage characterization reflects the notion that the rock matrix usually has a larger volume and fractures have a smaller volume. The two continua interact through fluid flowing from matrix to fractures.

The analytical solutions for pore-fluid pressure change in a dual porosity medium were derived for steady-state flow by Warren and Root (1963) and for transient flow by Kazemi (1969). Essentially, the pressure change in these systems is bounded by two Theis solution (Equation 6) shaped curves. At early time, the pressure change follows the behavior of high-permeability low-storage fracture media. Through time, the pressure change transitions and eventually conforms to the behavior of low-permeability high-storage matrix media (Figure 3 in Moench, 1984). A significant advancement in applying pore-pressure diffusion to studying induced seismicity is the introduction of hydraulic diffusion dependence on pore pressure, thus nonlinear pore-pressure diffusion (Shapiro & Dinske, 2009). The idea is that fractures generated during fracking under high injection pressure often remain open, supported by proppants, and the hydrologic properties of the fracked rock media are altered depending on the state of pore pressure. Shapiro and Dinske (2009) proposed a general nonlinear pressure diffusion equation and derived an expression for the seismicity triggering front in time and space. They found that the degree of nonlinearity affects propagation of the triggering front and creates more microseismicity.

Nonlinear pore-pressure diffusion represents a theoretical advancement in itself and demonstrates success in addressing questions concerning induced seismicity, for example, post-injection seismicity as discussed later in this article. The case examples, we present in the following, come from studies employed conventional linear pore-pressure diffusion.

2.2.2. Case Examples

2.2.2.1. Rocky Mountain Arsenal, Denver, CO, USA

Fluid injection induced seismicity in the Rocky Mountain Arsenal near Denver, CO, USA, is a classic example that serves as a reminder that history does repeat itself as wastewater injection induced seismicity in recent years bears similarity with this case. A series of earthquakes occurred in 1962 through 1965 when the wastewater, produced from the Rocky Mountain Arsenal, was injected into a granitic formation at a depth of 3,670 m. The injection operation halted in February 1966, but seismicity continued and three greater than magnitude 5 earthquakes occurred in 1967 (Hsieh & Bredehoeft, 1981). Evans (1966) observed the correlation between wastewater injection and seismicity and hypothesized that pore-fluid pressure increases, from fluid injection, reduced the effective normal stress across the fault so that the shear stress exceeded the shear strength of the already critically stressed fault, which is a mechanism proposed by Hubbert and Rubey (1959) to explain thrust faulting. Healy et al. (1968) applied the concept of Hubbert and Rubey (1959) to explain the seismicity occurrence at the Rocky Mountain Arsenal.

To further test the hypothesis, a fluid injection field experiment was conducted in the Rangely Oil Field in western Colorado (Raleigh et al., 1976), where water flooding through fluid injection, used for extracting oil, had already caused earthquakes recorded by a local network of seismometers. The year-long field experiment involved repeated fluid injection and flowback while monitoring seismicity by the local network and monitoring pore-fluid pressures in nearby wells. With measured in situ stresses and laboratory-measured friction properties, they predicted the pore-fluid pressure required to trigger earthquakes. The in situ pore-fluid pressure field was inferred from observed values in nearby wells and predicted by a computer model. By comparing the in situ and predicted pore-fluid pressure values, the experiment demonstrated and confirmed the predicted effect of pore-fluid pressure diffusion on triggering earthquakes, and it was further suggested that earthquakes can be controlled if the pore-fluid pressure in a fault zone can be manipulated at the injection well head (Raleigh et al., 1976).

Hsieh and Bredehoeft (1981) conducted a pore-fluid pressure diffusion modeling analysis that assumed a 30 km long and 3.35 km wide reservoir at a depth extending from 3.7 to 7 km below the land surface. They constrained the reservoir dimension and its hydraulic diffusivity at $\sim 1.0 \text{ m}^2 \text{ s}^{-1}$ using the field geologic and hydrogeologic data. The injection well was placed in the middle of the reservoir. The area of pore-fluid pressure buildup was compared to epicenter locations, showing that seismicity occurred within a zone in the reservoir, where pore-fluid pressure buildup exceeded 3.2 MPa. This was considered to be a critical pressure buildup value for triggering earthquakes at this site and consistent with the pore-fluid pressure range found from the Rangely field experiment (Raleigh et al., 1976). Hsieh and Bredehoeft (1981) then concluded that an increase in pore-fluid pressure was the trigger for the earthquakes at the Rocky Mountain Arsenal.

2.2.2.2. Raton Basin, Colorado-New Mexico USA

The Raton Basin in south-central Colorado and north-central New Mexico, exhibited low seismicity levels historically but has experienced a robust increase in seismicity since 1999, including an M_w 5.3 earthquake in 2011 (Barnhart et al., 2014; Meremonte et al., 2002; Rubinstein et al., 2014). The increase in seismicity coincided with a sharp increase in wastewater injection. Coal bed methane production in the Raton Basin since 1994 included dewatering operations that pumped a mixture of methane gas and pore water out of the production formation, yielding a large volume of wastewater once the gas is separated from the mixture. Injection of the wastewater in substantial quantities into the deeper part of the Basin started in 2001 (Weingarten, 2015). Rubinstein et al. (2014) suggested that such fluid injection is responsible for inducing most of the seismicity since 2001 in the Raton Basin. Studies have attributed the seismicity to fluid injection also because most of the seismicity occurred within a few kilometers of higher volume and higher rate injection wells. However, the seismicity predominantly occurred at depths between 2 and 6 km (Nakai et al., 2017), that is, below the major fluid injection interval of 1–2 km.

To better understand the vertical connection between injection and deeper seismicity, pore-fluid pressure diffusion modeling was conducted using MODFLOW (Nakai et al., 2017). The modeling incorporated vertical heterogeneity between the sedimentary formation, where the fluid was injected, and the deeper basement. Constrained by geology, hydrogeology, and seismicity, with data from 28 injection wells, the model suggested that pore-fluid

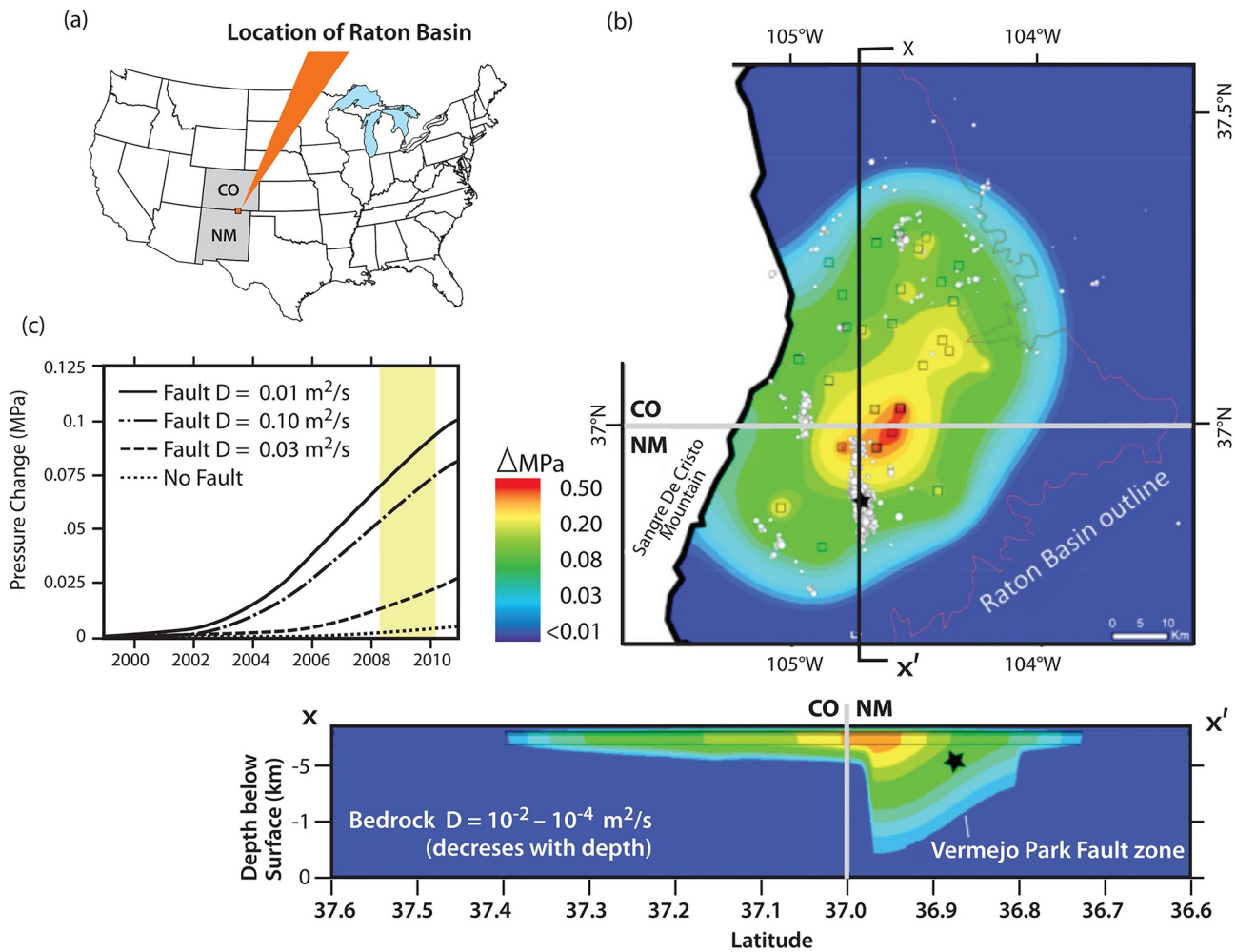


Figure 4. (Nakai et al., 2017). (a) Location of the Raton Basin in the USA. (b) Modeled pore-fluid pressure change in February 2020 in the injection Dakota formation in plan view and in the north-south cross section through the fault zone denoted by the solid line $x-x'$. The gray line is the boundary between the state of Colorado (CO) and New Mexico (NM). White dots indicate earthquakes. The black boundary in the west is the western extent of the Raton Basin. The brown line indicates the extent of the Raton formation at the land surface. Solid black lines in the cross section mark the hydrostratigraphic units. (c) Modeled pore-fluid pressure change versus time for varying fault zone diffusivity scenarios at a location in the fault marked by the black star in (b). The shaded yellow region represents the period of interest from 2008 to 2010 when the seismicity data were studied. The fault is modeled as a vertical homogeneous isotropic feature.

pressure increases, reaching 0.08 MPa in the seismicity zone, are broadly consistent in timing with the occurrence of a dominant seismic sequence (Figure 4). The modeled pore-fluid pressure increases provided further support for the argument that the seismicity surge in the Raton Basin was caused by subsurface fluid injection. In particular, the model demonstrated that high-permeability fault lineaments, inferred from seismicity, played a crucial role in facilitating pore-fluid pressure diffusion to depth, providing a mechanism that can explain the connection between fluid injection and deeper seismicity.

2.2.2.3. Soultz-sous-Forêts, France

In simulating pore-pressure diffusion induced seismicity at Soultz-sous-Forêts, Baisch et al. (2010) zoomed in on a fracture zone that intersects the injection well, into which fracking fluid was injected under pressure. Using a finite element model, they simplified the fault zone as a subvertical rectangle, but considered permeability enhancement due to slippage as seismicity occurs. Seismicity triggering is determined by the Coulomb failure criterion in a prescribed stress field. Their modeled spatial distribution of overpressures and its temporal evolution was capable of reproducing the main features of observed seismicity in terms of the number and magnitude of induced events and hypocenter locations. Moreover, post-injection seismicity, including the largest event, was

also explained and attributed to the continuing growth of the fluid pressure front in the fracture, such that the zone, where the fluid pressure increased, hosted the maximum seismic event.

2.3. Poroelasticity

2.3.1. Fundamentals

Poroelasticity studies the coupling between pore-fluid pressure and solid rock stresses, that is, how changes in solid rock stresses cause changes in pore-fluid pressure and vice versa (e.g., Wang, 2000). Poroelastic processes can include one-way solid-to-fluid or fluid-to-solid coupling or complex two-way coupling with feedbacks from solid to fluid and from fluid to solid. An observed poroelasticity phenomenon was well documented in 1892 at a farm near a train station in Wisconsin, where water levels in a well went up as trains were coming to the station and dropped back as trains were leaving the station (King, 1892). Here, the water levels in the well reflected changes in pore-fluid pressure in the rock formation and the train acted as a mechanical load that increased the stresses in the formation.

Theoretical treatment of poroelasticity was pioneered by Biot (1941) who introduced a pore-fluid pressure term into the stress-strain constitutive relation to take into consideration the influence of pore-fluid pressure on strain. For a more systematic treatment of the derivations of the coupled governing equations for pore-pressure diffusion and poroelastic stress equilibrium as well as detailed discussions of coupling hydromechanical parameters, readers are referred to the numerous existing sources (e.g., Rice & Cleary, 1976; Wang, 2000; Wang & Manga, 2021). Theoretical advancements were made in deriving analytical solutions for pore-fluid pressure and stress in simplified domain geometries under various boundary conditions as well as more rigorous definitions of coupling parameters (e.g., Cleary, 1977; Rice & Cleary, 1976; Rudnicki, 1986; Segall, 2010). Two sets of analytical solutions for pore-fluid pressure and poroelastic stresses by Rudnicki (1986) are most commonly used when studying induced seismicity (e.g., Goebel et al., 2017; Segall & Lu, 2015). One solution applies to a 3D half space under a point source and the other to a 2D radially symmetric domain under a line source under plane strain assumptions. The latter, similar to the analytical pore-fluid pressure diffusion solution (Equation 6), is given by Rudnicki (1986, Equations 12 and 51) as

$$P(\mathbf{x}, t) = \frac{q}{4\pi \left(\frac{k}{\gamma}\right) \rho} \int_u^\infty \frac{e^{-u}}{u} du, \quad u = \frac{r^2}{4Dt}, \quad D = \frac{\kappa(\lambda_u - \lambda)(\lambda + 2G)}{\zeta^2(\lambda_u + 2G)}, \quad (8)$$

where q is the injection rate per unit length ($\text{ML}^{-1}\text{t}^{-1}$), D is again the hydraulic diffusivity (L^2t^{-1}), and $\kappa = k/\gamma$, λ_u and λ are undrained and drained Lamé moduli ($\text{ML}^{-1}\text{t}^{-2}$), respectively. G is another Lamé modulus, also known as the shear modulus ($\text{ML}^{-1}\text{t}^{-2}$), $\zeta = 1 - K/K_s$ and K is the drained bulk modulus ($\lambda + \frac{2}{3}G$), and K_s is an experimental constant that for fully saturated media can be identified with the bulk modulus of the solid matrix (Rice & Cleary, 1976). It should be noted that in this theory the undrained shear modulus is the same as the drained shear modulus. It can be seen that the pore-fluid pressure solution from the coupled poroelasticity approach is identical to the pore-fluid pressure solution from well hydraulics, except that the hydraulic diffusivity, D , is defined with a more mechanical modulus in the poroelasticity approach than that in well hydraulics. Thus, one can expect that the pore-fluid pressure results from either pore-fluid pressure diffusion or poroelasticity produce similar solutions for this specific case. In general, there are several conditions under which pore-fluid pressure diffusion and poroelastic stress can be uncoupled, including the displacement field being irrotational (Detournay & Cheng, 1993; Verruijt, 2014, Chapter 1.10).

Note that Equations 6 and 8 are essentially the same, and yet they were derived from two seemingly different subdisciplines: well hydraulics and poroelasticity. Equation 6 is the solution to a special case in poroelasticity. By expanding the compressibility terms in Equation 6, the two expressions for diffusivity are also consistent.

Corresponding to the pore-fluid pressure solution Equation 8, the analytical solution for stress is (Rudnicki, 1986, Equation 52):

$$\sigma_{ij} = \frac{q\zeta G}{4\pi\rho \left(\frac{k}{\gamma}\right) (\lambda + 2G)} \left[\left(\delta_{ij} - \frac{2x_i x_j}{r^2} \right) \left(\frac{1 - e^{-u}}{u} \right) - \delta_{ij} \int_u^\infty \frac{e^{-u}}{u} du \right], \quad (9)$$

where i and j are directional indices for principal stresses, taking values of 1 and 2, and δ is the Kronecker delta.

Analytical solutions, such as those presented above, are straightforward to employ and often provide useful insights into system response or sensitivity to formation properties, even though they are limited to idealized conditions, such as a constant fluid injection rate and homogeneous rock properties. Studies that employed the poroelasticity approach often dealt with one-way fluid-to-solid coupling to focus on the stress field in rocks and how it is influenced by pore-fluid pressure changes due to fluid injection or extraction. In contrast, the feedback from rock stresses to pore-fluid pressures is considered secondary and is thus often ignored. Varying in degree of sophistication, numerical poroelasticity models have been developed and applied to studying injection induced seismicity (e.g., Fan et al., 2016; Shirzaei et al., 2016; Wang & Kämpel, 2003).

2.3.2. Case Examples

Poroelasticity theory has been applied to studying fluid-rock mechanical interactions prior to studying injection-induced seismicity. For example, poroelasticity effects were invoked to explain observed subsidence in fluid extraction settings, where reduced pore-fluid pressure caused compressional strain in the center of the basin triggering reverse faulting, but extensional strain on basin flanks triggering normal faulting (Segall, 1989; Segall et al., 1994), to assess fault stability under surface reservoir loading (e.g., Roeloffs, 1988), to study an increase in seismicity due to groundwater recharge spikes caused by spring snow melt (Christiansen et al., 2005; Saar & Manga, 2003), to investigate faulting-driven groundwater flow in sedimentary basins (e.g., Ge & Garven, 1992), induced seismicity and subsidence caused by oil and gas production in western Canada (Baranova et al., 1999), and to study fault interactions (Cocco & Rice, 2002). Renewed interests in utilizing poroelasticity theory to investigate injection-induced seismicity arose particularly from observations that are inexplicable by pore-fluid pressure diffusion.

2.3.2.1. Central Oklahoma, USA

Central Oklahoma, USA, has been “ground zero” for wastewater injection-induced seismicity. Three magnitude >5 earthquakes occurred in 2016 and are discussed in the following. One of them is the M_w 5.1 Fairview sequence that includes two seismicity clusters at 20–50 km from the initial seismicity and 10–40 km from subsurface fluid injection. These distances are considered beyond the extent of pore-fluid pressure diffusion influence. For a characteristic length for fluid pressure diffusion, defined by \sqrt{Dt} where D is hydraulic diffusivity and t is time, to be 10 km over 5 yr, the minimum diffusivity required is $1.0 \text{ m}^2 \text{ s}^{-1}$. Despite being within the range of diffusivity inferred from an event distance-time plot, in-situ and laboratory measured diffusivities are often much smaller (e.g., Doan et al., 2006; Kranz et al., 1990). Goebel et al. (2017) applied the poroelasticity analytical solutions of Rudnicki (1986), Equations 3 and 4, to evaluate the role of pore-fluid pressure diffusion and poroelastic stresses for a line-injection source in a 2D domain that is radially symmetric around the line source. A key point they demonstrated is that poroelastic stresses surpass the pore-fluid pressure in the far field and become the dominant factor for the Coulomb stress increases on the faults (Figure 5). While the value of poroelastic stress also depends on the fault orientation, the poroelastic stress is largely attributed to a broader, pressurized pore-fluid pressure source region, formed by a cluster of injection wells. The poroelasticity approach led them to conclude that pore-fluid pressure buildup in the range of 0.1–1 MPa likely induced seismicity near the fluid injection location, whereas poroelastic stresses probably triggered the far-field seismicity.

We note that there is no consensus on a definitive distance that constitutes far-field. The distance over which seismicity has been associated with fluid injection has evolved from about 5 km (Davis & Frohlich, 1993) to tens of kilometers (e.g., Keranen et al., 2014) to more than 100 km (e.g., Pollyea et al., 2018). In this article, we consider far field generally being beyond the influence of pore-fluid pressure diffusion from injection, which ranges from hundreds of meters in some theoretical or modeling studies to more than tens of kilometers in case examples.

Theoretically, the spatial influence of pore-pressure diffusion can be related to the characteristic length for pore-pressure diffusion \sqrt{Dt} . The values of D , however, can vary by several orders of magnitude for the upper crust. The D values inferred from a widely used approach, based on a seismic event distance-time plot (Shapiro et al., 1997), often fall within the range of 0.1–1 $\text{m}^2 \text{ s}^{-1}$ (e.g., Goebel et al., 2017; Molina et al., 2020; Shapiro et al., 2002) and can be orders of magnitude larger than those measured in the laboratory (e.g., Kranz et al., 1990) or in situ (e.g., Doan et al., 2006). Thus, it is necessary to be mindful that uncertainty in D values contribute to the uncertainty in estimating the characteristic length for pore-fluid pressure diffusion.

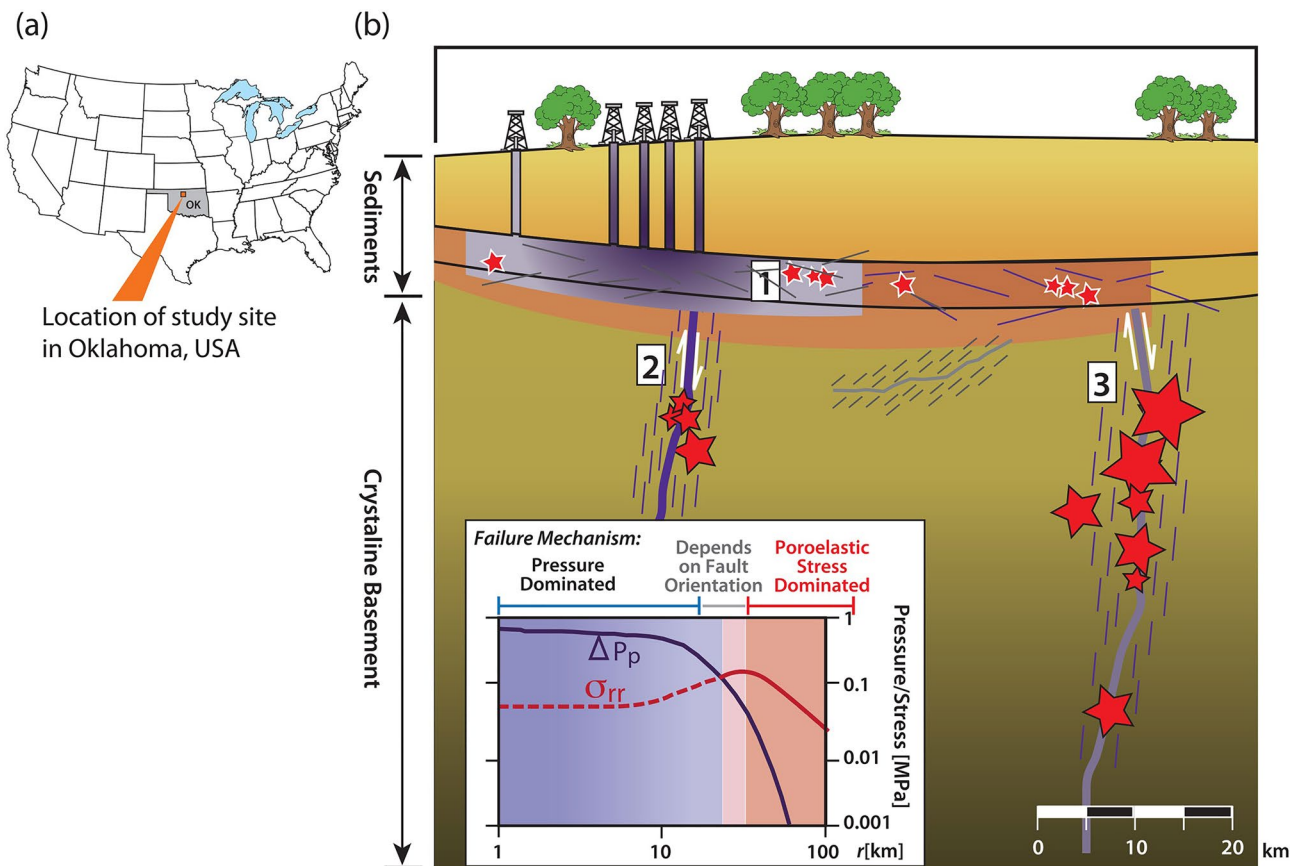


Figure 5. (a) Location of central Oklahoma. (b) Schematic comparison of the effects of pore-fluid pressure diffusion and poroelastic stresses on inducing seismicity. 1: near-injection pore-fluid pressure changes from diffusion dominate; 2: near-site faults can be weakened by the pore-fluid pressure diffusion; 3: far-field fault failure can be triggered by poroelastic stresses (Goebel et al., 2017).

While Goebel et al. (2017) demonstrated how poroelasticity theory was applied to examine stress changes from fluid injection and their influence on stress conditions at far distances, they linked volumetric poroelastic stress, not the Coulomb failure stress, to seismicity. Volumetric stresses do not explicitly reveal the sign and magnitude of Coulomb failure stress on fault. Fault orientations, relative to the directions of radial and tangential poroelastic stresses, could make the poroelastic stress either inhibit or promote slip (e.g., Segall, 1985; Segall & Lu, 2015; Zhai et al., 2019).

The 2016 M_w 5.8 Pawnee earthquake in central Oklahoma is the largest recorded earthquake associated with wastewater injection induced seismicity. Barbour et al. (2017) found that there were significant increases in the fluid injection rate in the years prior to the earthquake. They conducted a poroelasticity study to examine the effects of the variations in the fluid injection rate. A layered poroelasticity half-space model, with point-source fluid injection, was used (Wang & Kümpel, 2003). They found that shear and normal stress reductions on the fault, caused by poroelastic stress changes, were comparable to those due to pore-fluid pressure diffusion. While long-term injection stressed the fault toward failure, short-term variations and increases in the fluid injection rate provided a trigger for the earthquake when both poroelastic stresses and pore-fluid pressure diffusion effects are considered.

The 2016 M_w 5.0 Cushing earthquake sequence in central Oklahoma was studied by Zhai et al. (2019) using a similar layered poroelasticity approach with the model from Wang and Kümpel (2003) for a point source in a 3D half space. Considering two optimal conjugate fault orientations, they computed the pore-fluid pressure and poroelastic stress response to subsurface fluid injections since 1995 and predicted the seismicity rate using the rate-and-state friction law (Dieterich, 1994). They successfully reproduced the magnitude-time distribution of magnitude 3+ earthquakes observed in 2008–2017 in Oklahoma. They pointed out that while poroelastic stress

changes alone have a relatively small effect, adding poroelastic stress changes to pore-fluid pressure changes can substantially increase the seismicity rate. Deng et al. (2020) reached a similar conclusion from their poroelasticity modeling study of the 2016 M_w 5.0 Cushing sequence in Oklahoma.

The studies on induced seismicity in Oklahoma discussed above have assumed injection started under normal hydrostatic conditions. However, this region is within a broader under pressured middle continent of the USA (Nelson et al., 2015). Johann et al. (2018) introduced the concept of underground reservoir induced seismicity to explain the seismicity occurrence in 2013–2016 in central Oklahoma. Their conceptual model was motivated by the knowledge that the injection formation was initially under-pressured, the injection formation is highly porous and permeable, and seismicity largely occurred in the basement below the fluid injection interval. Thus, injected fluid could initially spread out within the permeable under-pressured injection formation above the basement, thereby adding weight and exerting loading on the basement, which is analogous to impoundment of surface reservoirs loading the rocks beneath the reservoir (e.g., Ge et al., 2009; Gupta, 2002; Simpson et al., 1988; Talwani, 1997). Johann et al. (2018) then used analytical and numerical solutions to examine pore-fluid pressure diffusion and poroelastic stress in the vertical direction and demonstrated that the underground reservoir induced seismicity model successfully explains the occurrences of seismicity in normal faulting and strike-slip settings that are common in central Oklahoma.

2.3.3. Influence of Local Tectonic Stress Field on Poroelastic Stress

The local tectonic stress field can affect Coulomb stress changes caused by poroelastic stresses. Altmann et al. (2014) provided the analytical basis for how different types of faults in a given tectonic stress field alter their Coulomb stress as pore-pressure changes. The basic idea is that changes in pore pressure and poroelastic stress, due to fluid injection or extraction, affect all components of the stress tensor on faults. How much change each stress component experiences depends on the fault orientation in the given tectonic stress field. For example, in a hypothetical but representative setting, during fluid injection, strike-slip and reverse fault regimes are more likely to reactivate faults oriented along the direction of the maximum horizontal stress, while normal fault regimes are more likely to reactivate faults in the vertical stress (Altmann et al., 2014).

The idea that the local tectonic stress field affects Coulomb stress changes on faults was well demonstrated by Goebel et al. (2017, Figure 8). They showed that the Fairview and Woodward faults in central Oklahoma experienced increased Coulomb stresses because their orientations were favorable for an increase in differential stresses in the local tectonic stress field.

2.4. Coulomb Static Stress Transfer

2.4.1. Fundamentals

Coulomb static stress transfer is another mechanism, that is, gaining traction when studying induced seismicity. Its theoretical basis is rooted in solving for stress changes in response to a dislocation in a half space elastic medium (Okada, 1992). The idea was proposed and applied to studying natural earthquake sequences, such as the 1992 Landers earthquake (King et al., 1994; Stein, 1999). To examine how one earthquake may contribute to triggering others, King et al. (1994) computed stress field change in a uniform half space in response to a slip on a fault that they named master fault. The stress field change from the slip on the master fault can be used to compute the changes in the normal and shear stress components of the Coulomb stress on other faults of known orientation in the vicinity of the master fault. This is the essence of the Coulomb static stress transfer mechanism, that is, slip along a fault results in static stress changes in regions around the fault, triggering more earthquakes on nearby faults, where the Coulomb stress is increased. Coulomb static stress transfer can either promote or inhibit earthquake triggering on existing faults (e.g., Stein, 1999, 2005; Toda et al., 2011), depending on the induced change of shear and normal stresses on the nearby faults. Coulomb static stress change (ΔCSS) is calculated (Stein, 1999) as

$$\Delta CSS = \Delta \tau_s + \mu (\Delta \sigma_n + \Delta P), \quad (10)$$

where $\Delta \tau_s$ is the shear stress change (positive when increased in the direction of fault slip), μ is the average friction coefficient of a fault, $\Delta \sigma_n$ is the change in normal stress (positive for extension, i.e., when the fault is

unclamped), and ΔP is the change in pore-fluid pressure in the fault zone (positive indicates a pressure increase). If only seeking the static stress change on faults of known orientation, the background stress is not required.

To compute ΔCSS on a fault, the location and parameters of the fault as well as the location and parameters of earthquakes around the fault are required. Fault parameters include fault orientation, dip, and depth. Earthquake parameters include magnitude, rupture length, rupture width, average slip, and slip direction. Coulomb 3, a USGS software (Lin & Stein, 2004; Toda et al., 2005, 2012) was developed for computing ΔCSS with built-in empirical relationships between earthquake magnitude and earthquake parameters (Wells & Coppersmith, 1994) for earthquakes with $M > 4.5$. For smaller-magnitude earthquakes, alternative relations to determine earthquake parameters, developed by Leonard (2010), have been applied (Brown & Ge, 2018b).

2.4.2. Case Examples

To assess the relative importance of the Coulomb static stress change from prior earthquakes and pore-fluid pressure diffusion, Brown and Ge (2018b) conducted a modeling study that examined Coulomb static stress effects on two idealized fault scenarios, a vertical strike slip fault and a normal fault in a 3D half space. The earthquakes were generated using the magnitude-frequency relation with varying b values (Gutenberg & Richter, 1944). Pore-fluid pressure modeling was conducted with an injection well in a 3D space using a range of fluid injection rates and hydrogeologic parameters. Comparing the results of modeled pore-fluid pressures and Coulomb static stresses, they found that the region influenced by pore-fluid pressure diffusion in general is larger than that of positive Coulomb static stress transfer, but the maximum Coulomb static stress changes are comparable, or larger than, the maximum pore-fluid pressure increase. Therefore, they suggested that small earthquakes, that generated Coulomb static stress changes, do matter when studying induced seismicity and that this is one of the triggering mechanisms that deserves attention.

2.4.2.1. Central Oklahoma, USA

The 2011 M5.7 Prague earthquake in central Oklahoma, USA, occurred 1 day after a M5.0 event. This motivated a study by Sumy et al. (2014) to investigate the role Coulomb static stress transfer, from the foreshocks, may have played in triggering the main shock. They detected and located 110 earthquakes in the sequence and resolved the Coulomb static stress change following an M5.0 foreshock. They found that 60% of the earthquakes following the M5.0 event, including the M5.7 mainshock, occurred on faults that experienced increased Coulomb stresses greater than 0.01 MPa, including the M5.7 mainshock. Observing that some of the detected earthquakes occurred in zones of negative Coulomb static stress change, primarily within 2.5 km of the ruptured portion of the fault plane, they recognized the limitation of the Coulomb static stress mechanism and attributed the seismicity to stress heterogeneity on fault planes in the complex Wilzetta fault system.

Approximately 110 km north of Prague occurred the 2016 M5.8 Pawnee sequence that bears some similarity to the Prague sequence (Chen et al., 2017). Foreshocks were observed to have propagated toward the mainshock. Two foreshocks with magnitudes greater than 3.5 occurred along the conjugate fault of the mainshock fault in the same Labette fault system. Additionally, two clusters of foreshocks occurred. Chen et al. (2017) computed the Coulomb static stress transfer from $M > 3$ foreshocks and found that they contributed positive CSS changes to the failure stress of the mainshock. One M3.7 foreshock produced a CSS of ~ 0.06 MPa, which is comparable to, or larger than, the injection-induced pore-fluid pressure or poroelastic stress changes modeled by Barbour et al. (2017). Thus, Chen et al. (2017) concluded that regional tectonic faults controlled the spatial distribution of the earthquakes, whereas the CSS transfer from fluid-injection induced foreshocks contributed to the 2016 M5.8 Pawnee mainshock.

2.4.2.2. Pohang, Korea

The 2017 Pohang M_w 5.5 earthquake at an EGS exploration site near the city of Pohang in South Korea was the largest-magnitude earthquake known to be associated with EGS operations (Figure 6a). In January 2016, the Pohang EGS project started hydraulic fracturing operations in two exploration wells, drilled to a depth of 4,200 m into granitic bedrock. Five hydraulic fracturing stimulations were conducted alternately in these two wells and earthquakes followed each stimulation, including a M_w 3.2 event on 15 April 2017. The M_w 5.5 mainshock occurred on 15 November 2017, 2 months after the last stimulation. Seismologic, geomechanic, and hydrogeologic studies as well as analyses of drilling data converged to the consensus that the earthquakes were induced. Specifically, a picture emerged suggesting that the pore-fluid pressure increase, from subsurface fluid

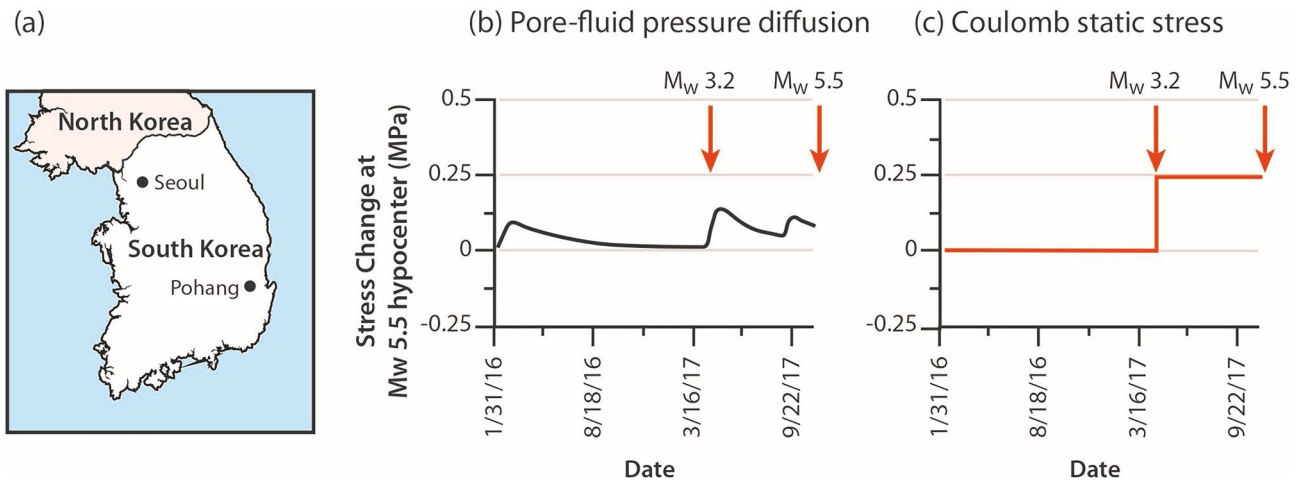


Figure 6. (a) Location of Pohang in South Korea. (b) Temporal evolution of modeled pore-fluid pressure diffusion. (c) Coulomb static stress on the fault of the mainshock at the Pohang EGS site (after Yeo et al., 2020).

injection, first induced a series of earthquakes on a pre-existing fault (hydraulic shearing), which eventually led to a weakening of the fault and the triggering of the mainshock (Ellsworth et al., 2019; Grigoli et al., 2018; Kim et al., 2018). However, the case is not quite closed yet, as efforts continue to describe and quantify the processes that operated at the site, leading to the mainshock (e.g., Chang et al., 2020; Yeo et al., 2020).

Yeo et al. (2020) modeled pore-fluid pressure diffusion and Coulomb static stress change. They used 59 $M_w > 0.3$ relocated earthquakes and their focal mechanisms from Ellsworth et al. (2019) and computed the spatiotemporal evolution of the Coulomb static stress transfer. For a Young's modulus range of 50–80 GPa, the Coulomb static stress change showed that 60%–70% of the 59 earthquakes occurred in regions with positive Coulomb static stress change and 40%–60% occurred in regions, where the calculated Coulomb static stress change was greater than 0.01 MPa. The change was 0.02–0.04 MPa at the M_w 3.2 foreshock hypocenter and 0.13–0.15 MPa at the M_w 5.5 mainshock hypocenter. Particularly noteworthy is that the M_w 3.2 foreshock caused a sharp increase in the Coulomb static stress at the mainshock hypocenter. Moreover, the Coulomb static stress change at the mainshock hypocenter exceeded the modeled pore-fluid pressure change (Figures 6b and 6c). Thus, they suggested that a causal mechanism for the mainshock is that pore-fluid pressure changes from pore-fluid pressure diffusion initiated seismicity on critically stressed faults and that Coulomb static stress transfer from the initial seismicity promoted more seismicity that included the mainshock.

2.5. Aseismic Slip

2.5.1. Fundamentals

Aseismic slip is often identified to accompany pore-fluid pressure diffusion when fluids are injected underground (Cornet, 2016) and to play a role in triggering larger earthquakes (Bourouis & Bernard, 2007; Wei et al., 2015). The idea of aseismic slip inducing seismicity was demonstrated by the in situ experiments at the Low-Noise Underground Laboratory in southeastern France (Figure 7a; Guglielmi et al., 2015). Fluid injection induced slips on a fault were documented while the pore-fluid pressure was monitored. As shown in Figure 7b, the pore-fluid pressure gradually builds up with subsurface fluid injection, which is followed by aseismic slip and displacement on the fault. Eventually, fault slip accelerates, leading to seismicity. Guglielmi et al. (2015) further observed that aseismic slip propagates faster than pore-fluid pressure diffusion, thereby affecting larger regions than pore-fluid pressure diffusion, which was also observed at the Soultz-sous-Forêts geothermal field in France (Cornet et al., 1997). The spatiotemporal evolution of pore-fluid pressure changes and fault slip shows that while fluid injection initiates aseismic slip, the faster propagation, and larger extent of the influence of aseismic slip could help explain seismicity in the far-field from fluid injection sites (Bhattacharya & Viesca, 2019).

We note that aseismic slip creates static stress transfer onto nearby faults, and is, thus, mechanically similar to Coulomb static stress transfer discussed in the preceding section. While Coulomb static stress transfer has

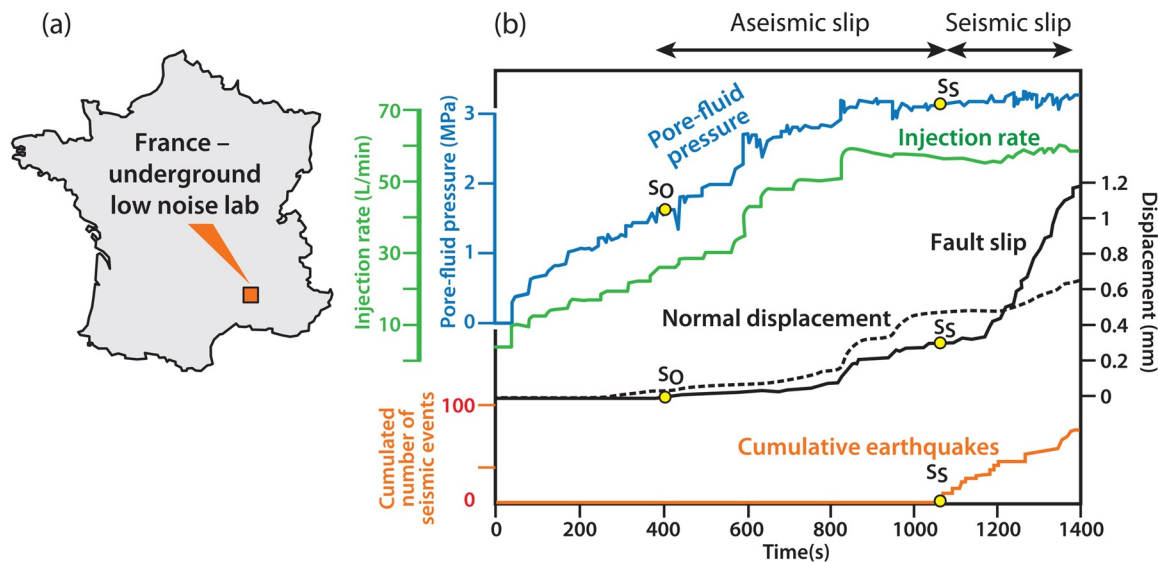


Figure 7. (a) Location of the Underground low-noise lab in southern France. (b) Illustration of aseismic slip leading to earthquakes (after Guglielmi et al., 2015). Pore-pressure builds up initially (blue line) with subsurface fluid injection (green line). At the time marked by S_0 , aseismic slip begins, and fault displacement and slip were recorded (dotted and solid gray lines). When the time reaches S_s , the fault slip accelerates, so does the seismicity (orange line), which leads to seismicity in the far field from the fluid injection location.

conventionally been invoked when discussing stress transfers from foreshocks to major earthquakes (e.g., King et al., 1994), aseismic slips drive similar static stress transfer. Studying aseismic slips, leading to induced seismicity in controlled experimental settings, has implications to understanding the details of fault mechanical behavior in fluid-driven earthquake tremors in natural settings (Bhattacharya & Viesca, 2019).

Similar to tectonic stresses ultimately controlling induced earthquake magnitudes, tectonic stress conditions prior to fluid injection control whether aseismic slip outpaces pore-pressure diffusion. As demonstrated by Bhattacharya and Viesca (2019), for critically stressed faults, aseismic slip outpaces pore-pressure diffusion, that is, aseismic slip occurs beyond the characteristic length of pressure diffusion. A similar result was presented by Sáez et al. (2021) for axisymmetric pressure diffusion and rupture propagation.

Critically stressed faults tend to exhibit higher permeabilities than non-critically stressed faults, based on borehole data from fractured and faulted crystalline rocks (Barton et al., 1995) and from deep drilling and induced seismicity experiments at crustal scales (Ito & Zoback, 2000; Townend & Zoback, 2000). This results in an interesting dichotomy. On the one hand, high permeability faults make the crust strong by transmitting fluids and by maintaining hydrostatic fluid pressure conditions in the crust (Townend & Zoback, 2000). On the other hand, high permeability faults preferentially channel fluids into faults, leading to higher pore pressures in these faults (e.g., Zhang et al., 2013), making themselves more susceptible to failure. We note that permeability is not the only factor determines hydraulic diffusivity, because permeable faults in the crust can be accompanied by damage zones of higher storage, but elevated permeability are often dominant over elevated storage. As for aseismic slip, faster pore-fluid pressure diffusion in more permeable faults probably outpaces aseismic ruptures across various tectonic settings.

2.5.2. Case Examples

Wei et al. (2015) reported the 2012 Brawley earthquake swarm near a geothermal power plant in the Imperial Valley in southern California, USA, including the largest M_w 5.4 event. The hypocenters at 4–9 km depth are much deeper than the fluid injection depth of 0.6–1.5 km. Aseismic slip was inferred from asymmetric land surface deformation around a shallow normal fault with subsidence on one side and uplift on the other, measured by leveling measurements, UAVSAR imaging radar, and Interferometric Synthetic Aperture Radar (InSAR). The aseismic slip occurred over a period of ~ 2 yr prior to two $M_w \geq 5.3$ events. Wei et al. (2015) suggested that the aseismic slip was initiated by a rapid increase in the subsurface fluid injection rate and that the aseismic slip subsequently triggered the main earthquake swarm. To understand how aseismic slip triggering works, they

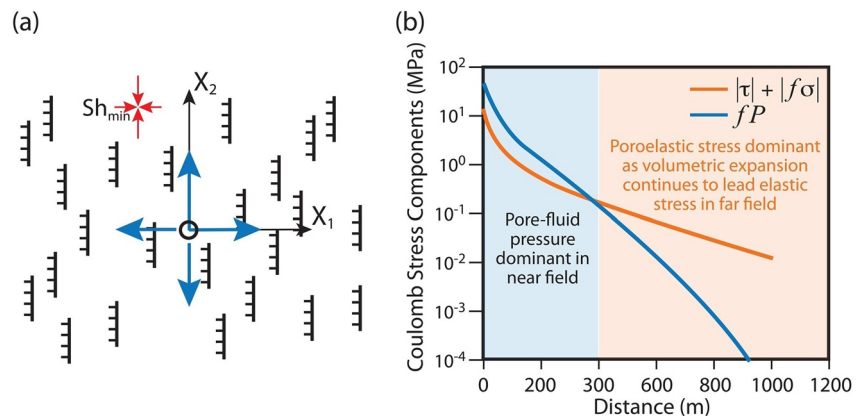


Figure 8. (After Segall & Lu, 2015). (a) Map view of the problem setup. Fluid injection is centered on a set of N-S striking normal faults with a dip of 60° to the west. The least principal horizontal compressive stress is normal to the fault strike. (b) Coulomb stress component change with distance from the fluid injection location at time = 5 days, due to pore-fluid pressure diffusion (blue line) and due to poroelastic stress (red line), where f is the friction coefficient. Close to the subsurface fluid injection location, pore-fluid pressures, due to diffusion (blue line), dominate. In the far field, poroelastic stress (red line) dominates because the volumetric expansion continues to create stresses.

modeled the Coulomb static stress transfer and found that the swarm started in regions of positive Coulomb static stress change, caused by the aseismic slip. This case study practically tied the aseismic slip and Coulomb static stress transfer triggering mechanisms.

3. Emerging Consensus on Outstanding Issues

3.1. Far Field Seismicity

Induced seismicity has occurred at places far from fluid injection wells and at places beyond the expected distance for pore-fluid pressure diffusion over reasonable time scales. Why? As illustrated in the examples above, poroelastic stresses, Coulomb static stress transfer, and aseismic slip have been invoked to address this question. Despite the theoretical and modeling studies discussed above, we are yet to learn about cases, where far-field seismicity can be exclusively attributed to poroelastic stress changes. Below is a generic poroelasticity study that sheds further light on this conundrum.

Exploring the effects of poroelastic effects and earthquake nucleation on seismicity rates, Segall and Lu (2015) used the analytical solution of Rudnicki (1986) to determine the poroelastic stresses and the pore-fluid pressure in a homogeneous 3D half space from a point-source fluid injection. The study domain is idealized to have the least horizontal stress strike east-west and is populated with a set of uniform faults striking north-south and dipping 60° to the west (Figure 8a). Translating the pore-fluid pressure and poroelastic stresses to Coulomb stress changes on those faults, they predicted a seismicity rate using a rate-and-state model (Dieterich, 1994). Figure 8b shows how Coulomb stresses change with distance eastwards from fluid injection. Close to injection, the effect of pore-fluid pressures dominates, due to pressure diffusion. In contrast, poroelastic stresses dominate in the far field because volumetric expansion continues to accumulate strain, thereby increasing stresses. While the Coulomb stress decreases with distance from the injection, due to both pore-fluid pressure and poroelastic stress decreases, these two decreasing trend lines cross at a distance, indicating their relative significance switches. Thus, despite small pore-fluid pressures in the far field, seismicity could occur as a result of poroelastic stresses. Furthermore, seismicity rates can change by orders of magnitude because of their exponential dependence on stress.

The hydrogeologic role of faults, being either conduits or barriers, in pore-pressure diffusion and fluid transport has long been recognized and debated (e.g., Ball et al., 2010; Bredehoeft et al., 1992; Caine et al., 1996). Studying far field seismicity, particularly those that occurred several kilometers deeper than the fluid injection interval, has renewed the discussion on what role faults play in inducing seismicity in various settings. Most treated faults as more permeable than surrounding rocks for enhancing pore-pressure diffusion. Below are a few examples.

Pore-pressure modeling by Zhang et al. (2013) suggested that permeable faults effectively extend the depth of pore pressure increase by several kilometers. Simulating the presence of normal and thrust faults in the basement, their modeled overpressure zones are consistent with the main spatial features of seismicity in Ohio and central Arkansas.

Hornbach et al. (2015) studied a series of felt earthquakes near Azle, Texas, where there are both hydrocarbon production and wastewater injection activities. They hypothesized that a permeable fault system in a low-permeability basement transferred pressure from hydrocarbon production and wastewater injection downward and contributed to the stress changes at the felt earthquake locations.

Goebel et al. (2016) examined the role of seismically active faults in inducing seismicity in southern Central Valley in California, where there is abundant natural background seismicity. On the basis of a detailed seismicity analysis and hydrogeological modeling, they suggested a connection by a permeable pathway of >10 km between high-rate wastewater disposal and the 2005 White Wolf earthquake sequence that had a maximum magnitude of M_w 4.6.

Modeling studies coupling pore pressure and poroelastic stress further elaborate the effects of permeable faults as hydrologic conduits in enhancing pore-pressure diffusion, thereby elevating pore pressures in faults that are far from fluid injection locations (e.g., Chang & Segall, 2016; Fan et al., 2019). They also emphasized the combined effects of poroelastic stress influence on Coulomb stress changes on faults for various fault orientations and tectonic regimes. Moreover, for basement faults that are hydrologically isolated and far from fluid injection intervals, modeling studies suggest that poroelastic stresses, transmitted to those faults, can cause sufficient Coulomb stress change to induce seismicity (Chang & Segall, 2016; Zhai et al., 2021).

The above discussion offers one explanation for inducing far-field seismicity, but no consensus on the cause of far-field seismicity has been reached. Take the Fairview earthquake sequence in Oklahoma, for example, while poroelastic stresses reached far-field distances (i.e., Goebel et al., 2017), Yeck et al. (2017) suggested that pore-fluid pressure diffusion from a cluster of high-rate fluid injection wells was the primary reason for causing seismicity. Moreover, Zhai et al. (2019) called for a comprehensive assessment of the effect of pore-fluid pressure diffusion from all fluid injection wells, low and high injection rates, near and far from seismic events, because pore pressure changes from near-field, low-rate fluid injection can also be significant. They suggested that pore-fluid pressure diffusion from fluid injections in Oklahoma could have caused seismicity in Kansas in the south (Peterie et al., 2018), when the importance of pore-fluid pressure diffusion from near-field, low-rate wells was considered (Zhai et al., 2020).

3.2. Post-Fluid Injection Seismicity

The largest events in induced seismicity sequences have often occurred after the fluid injection periods at both wastewater injection and hydraulic fracturing sites. For example, at the Rocky Mountain Arsenal site, discussed in Section 2.1.2, three magnitude >5 earthquakes occurred several months after fluid injection had stopped. Delays ranging from months to years between the reduction in the fluid injection rate and the seismicity rate were also reported in Oklahoma (e.g., Goebel et al., 2017; Keranen et al., 2013) and Texas (e.g., Ogwari et al., 2018), USA. Post-injection seismicity at EGS sites include Basel in Switzerland, Soultz-sous-Forêts in France, and Berlin in El Salvador. In Basel, the largest event (M_L 3.4) occurred after the fluid injection stopped, although the time lag was less than 1 day (Deichmann & Giardini, 2009; Häring et al., 2008). At Soultz-sous-Forêts, larger earthquakes occurred days after shut-in (Charl  ty et al., 2007). At the Berlin geothermal field, the largest event (M_L 4.4) occurred 2 weeks after shut-in (Bommer et al., 2006).

Post-fluid injection seismicity was also reported for hydraulic fracturing operations in shales in western Canada, where the largest event of M_w 3.9 occurred 2 weeks after completing hydraulic fracturing, during the flow-back period (Bao & Eaton, 2016). In a geothermal field at Brady Hot Spring, NV, USA, seismicity increases were observed to correlate with fluid extraction rate changes both increasing to above its long-term average and decreasing to zero during shutdown, which was hypothesized to be a reaction of the subsurface effective stress field that has adapted to the long-term average condition (Cardiff et al., 2018).

Segall and Lu (2015) offer an explanation from a poroelasticity perspective. They note that poroelastic stresses, during fluid injection, could either promote or inhibit fault slip, depending on the fault orientation relative to

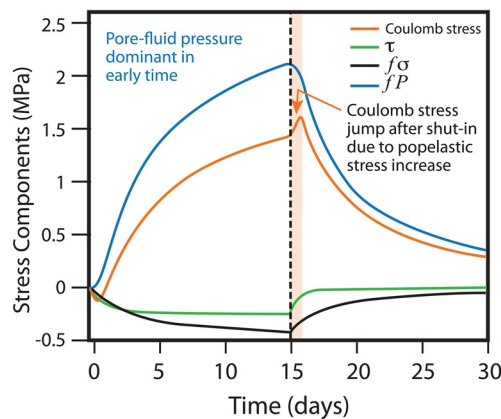


Figure 9. (After Segall & Lu, 2015). Poroelasticity explanation for post-fluid injection seismicity. During subsurface fluid injection at $X_1 = 200$ m and $X_2 = 0$ (coordinate notation is shown in Figure 8), the Coulomb stress component on a fault, due to the increase in pore-fluid pressure, increases (blue line), whereas the Coulomb stress component on the same fault, due to poroelastic stresses, decreases (green and gray lines). Thus, during fluid injection, the total Coulomb stress on the fault (orange line) increases. After shut-in, pore-fluid pressure diffusion continues and poroelastic stresses start to increase. The resulting total Coulomb stress (orange line) increases (pink bar region) before it declines.

the injector. For example, poroelastic stresses promote slip on the N-S striking normal faults shown in Figure 8a during fluid injection but inhibit slip post-injection; and poroelastic stresses on strike-slip faults with fault normal radial to the point-source fluid injector would be compressional during fluid injection. Faults that are inhibited during fluid injection would experience post fluid injection relaxation of the compressive stresses across the faults, while the diffusion of the pore-fluid pressure continues, which promotes seismicity.

These findings elegantly demonstrate the utility of poroelasticity in explaining post shut-in occurrences of seismicity. As shown in Figure 9, during fluid injection, for the arbitrary fault specified in their study (Figure 8a), the Coulomb stress on the fault increases due to pore-fluid pressure diffusion. At the same time (during fluid injection), the Coulomb stress decreases due to changes in poroelastic stresses. The total Coulomb stress on the fault, adding these two effects, increases during fluid injection. After shut-in, during a narrow time window, pore-fluid pressure diffusion continues, so that the pore-fluid pressure continues to increase, while poroelastic stresses start to increase. The result is a sharp increase in total Coulomb stress, marked by the small upwards bump of the red curve in Figure 9. Consequently, seismicity after shut-in can increase. Segall and Lu (2015) suggested that the more abrupt a shut-in is, the sharper the Coulomb stress increase is, thus, smoothly tapering off the subsurface fluid injection rate could reduce induced seismicity.

A noteworthy study tackling post-injection seismicity was conducted by Johann et al. (2016) who applied nonlinear pore-pressure diffusion concept (Shapiro & Dinske, 2009) to examine post-injection phenomena. This study is based on the method developed by Rothert and Shapiro (2003) and the hypothesis that preexisting critically stressed fractures are triggered by small perturbations of pore-fluid pressure. Johann et al. (2016) derived a scaling law for the triggering front and back front of induced seismicity. The triggering front represents the upper distance bound of the seismicity cloud. The back front, starting at the time when the injection stops, represents the lower distance bound of the seismicity cloud. These two fronts, thus, predict the spatiotemporal evolution of seismicity. Johann et al. (2016) showed that post-injection seismicity occurrence is influenced by the degree of nonlinearity in pore-pressure diffusion (Shapiro & Dinske, 2009).

3.3. Injection Rate Culpability

Seismicity data and injection data from 34 states in the east-central USA over the past four decades revealed that seismicity is spatiotemporally correlated to high fluid injection rate wells (Weingarten et al., 2015). Zooming in on north-central Oklahoma, Pollyea et al. (2018) conducted a geospatial analysis of earthquake centroids and injection volume weighted well centroids using data from 2011 to 2016, and found that these two centroids are spatially cross-correlated to a length scale of 125 km. A higher injection volume in the Pollyea et al. (2018) study can be viewed as a high injection rate because of the short duration of the operation of a few years. Cochran et al. (2018) linked the rapid rise in seismicity in southern Kansas to high-rate injection wells by developing and analyzing the timing and location of seismic events from 2014 to 2017.

Alghannam and Juanes (2020) used rate-and-state friction with a spring-slider analog to study the poroelastic behavior of earthquake nucleation and analyzed conditions for fault instability. A steady slip rate is represented by a moving spring that pulls a slider, a system that reflects the poroelastic deformation and pore-fluid pressure diffusion driven by the fluid injection, as well as the poroelastic coupling between the shear and effective normal stresses along a fault. The rate-and-state law dictates that the shear strength is a function of the effective normal stress and of the friction coefficient, which varies with slip rate and the state of the sliding surface. As fluid injection changes the effective normal stress, the friction coefficient is coupled through a poroelastic model of pore-fluid pressure and rock deformation.

A key finding of Alghannam and Juanes (2020) is that the rate of pore-fluid pressure increases, hence the rate of effective normal stress reduction, matters more than the magnitude of the pore-fluid pressure increase. They suggest that, for a given volume of injected fluid, a high fluid injection rate over a shorter period of time increases the seismic risk, compared to a lower rate over a longer period of time, as large increases in the fluid injection rate tend to intensify seismicity at early times. Their findings support the notion that the fluid injection rate is the operational parameter, that is, more likely to induce seismicity (Weingarten et al., 2015) and offer practical guidance for injection strategies to mitigate seismicity risks.

3.4. Fluid Injection Volume and Maximum Earthquake Magnitude

McGarr (2014) proposed that the maximum magnitude of earthquakes induced by fluid injection is controlled, or bounded by, the cumulative injection volume. The abundance in seismicity and widespread fluid injection activities afford an opportunity for in-depth examinations on how well this idea holds. McGarr and Barbour (2017) examined three induced earthquakes in Oklahoma in 2016 that exhibited different characteristics in their foreshock and aftershock sequences. The M5.1 Fairview earthquake exhibited extensive foreshocks and aftershocks. The M5.8 Pawnee earthquake showed few notable foreshocks or aftershocks. The M5.0 Cushing earthquake was accompanied mainly by foreshocks. Yet, the seismic moment releases of these sequences, thus their maximum magnitudes, were limited by the injected fluid volumes to within 10 km of the main events (McGarr & Barbour, 2017).

The premise of a fluid injection volume versus earthquake magnitude relation has been challenged by others. For example, van der Elst et al. (2016) studied 19 fluid injection induced seismicity sites around the world and observed that the largest earthquakes fit the magnitude-frequency distribution for tectonic earthquakes without an upper bound and occurred randomly during the induced sequence. They argued that fluid injection controls earthquake nucleation, but tectonics controls the magnitude. The 2017 Pohang earthquake also clashed with McGarr's (2014) fluid injection volume versus earthquake magnitude relation, as the magnitude is nearly two units larger than the volume-based prediction, that is, for a M_w 5.5 earthquake, the injected fluid volume would need to be much greater than what was injected at Pohang. The Pohang earthquake not only exceeded the maximum earthquake magnitude predicted, due to the injection of a given fluid volume, by McGarr (2014) but also the maximum magnitude predicted by others (Galis et al., 2017; van der Elst et al., 2016). In this regard, Pohang was an exception to any existing maximum magnitude estimations. Ellsworth et al. (2019) showed that the magnitude of the 2017 Pohang earthquake has more to do with tectonic stresses than with the volume of the injected volume.

It suffices to say that a volume-magnitude relationship remains controversial, or at least a topic of continuing research (e.g., Galis et al., 2017; van der Elst et al., 2016), and caution needs to be exercised when applying it to predict the maximum magnitude of fluid-induced seismicity.

3.5. Hydraulic Stimulation Implicated

Wastewater injection, not hydraulic stimulation, has been deemed the main culprit for the sharp increase of induced seismicity over the past decade, despite the public misconception that equates hydraulic stimulation with earthquakes. Felt or damaging seismicity, induced by hydraulic stimulation, remains uncommon. Increasingly, cases are reported where felt earthquakes were linked to hydraulic stimulation operations at EGS sites and in oil and gas reservoirs. For example, an M_L 2.3 event was reported in Lancashire, England (Clarke et al., 2014), an M_L 3.0 in Ohio, USA (Skoumal et al., 2015), an M_w 3.9 in Alberta, Canada (Schultz et al., 2015; Bao & Eaton, 2016), and an M_w 4.6 in British Columbia, Canada (Mahani et al., 2017). Shapiro et al. (2011) suggested that differences in stimulated rock volumes in geothermal and hydrocarbon reservoirs contributed to observed differences in seismicity magnitude.

The 2017 M_w 5.5 earthquake at the Pohang EGS site in Korea is the latest such example. The Basel case in Switzerland is the first case, where significant seismicity was related to hydraulic stimulation at an EGS development site, with the largest earthquake being an M_L 3.4 event in 2006–2007 (Deichmann & Giardini, 2009; Häring et al., 2008). The pore-fluid pressure in the formation did not reach the least compressive stress necessary for hydraulically stimulating the rock (Häring et al., 2008) and most of the seismicity occurrence did not

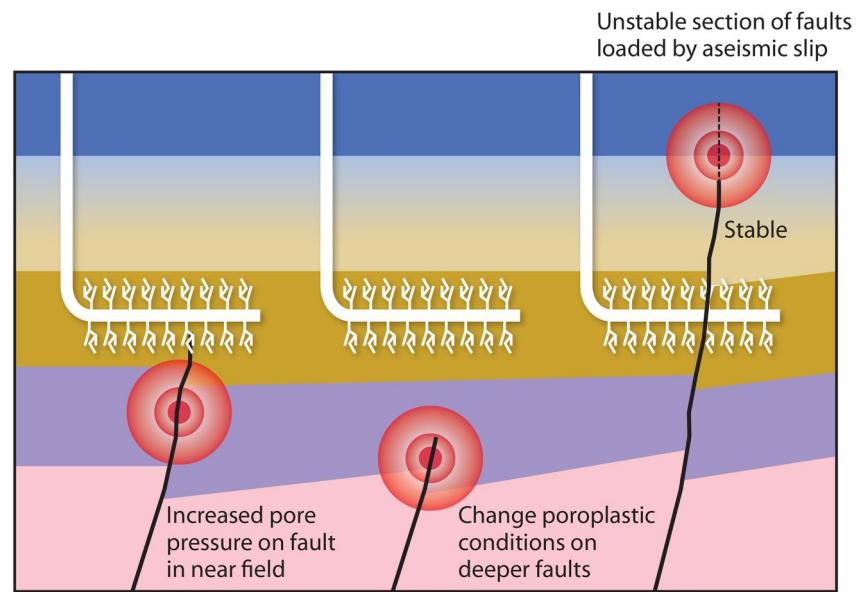


Figure 10. (After Eyre, Eaton, Garagash, et al., 2019). Schematic representation illustrating fault activation and induced seismicity by hydraulic fracturing in shale gas reservoirs. 1. An increased pore-fluid pressure reduces the fault strength. 2. The pore-elastic stress loads the fault, causing slip. 3. The pore-fluid pressure initiates aseismic slip along the fault and triggers distal earthquakes.

coincide with the maximum well-head pressure. Pore-fluid pressure increases from fluid injection were attributed to triggering the earthquakes on pre-existing faults by decreasing the effective stress, but the background tectonic stress was thought to be the driving factor (Deichmann & Giardini, 2009).

Hydraulic fracturing of oil and gas reservoirs is distinct in that pore-fluid pressure diffusion in low-permeability shale formations is significantly inhibited. The characteristics of pore-fluid pressure propagation could differ substantially from other operations, where fluids are injected into more permeable formations (Atkinson et al., 2016; Bao & Eaton, 2016). Pore-fluid pressure buildup, from fluid injection into low-permeability zones, could be larger than that in more permeable formations, however, the spatial extent of pore-fluid pressure propagation is more limited. Consequently, the fault-activation process in shale is less clear as faults may lie outside the influence zone of pore-fluid pressure diffusion (Bao & Eaton, 2016). Citing reported cases from Canada (Eaton et al., 2018; Eyre, Eaton, Zecevic, et al., 2019; Mahani et al., 2017) and Ohio, USA (Skoumal et al., 2015). Eyre, Eaton, Garagash, et al. (2019) observed that earthquakes are vertically offset from, and below the horizon of, hydraulic fracturing locations. Three hypotheses are illustrated in Figure 10. One involves increased pore-fluid pressures in the fault zone, leading to a reduction of the effective normal stress on the fault. Another hypothesis states that poroelastic stress loading causes the fault to slip. The third hypothesis invokes pore-fluid pressure initiated aseismic slip to trigger distal earthquakes. These hypotheses are well supported by a number of studies (e.g., Bao & Eaton, 2016; Clarke et al., 2014; Elsworth et al., 2016; Schultz et al., 2015, 2017).

3.6. Geodetic Data as Model Constraints

When studying induced seismicity, models of pore-fluid pressure diffusion and geomechanics have faced challenges when calibrating the models because of scarcity in direct measurements of pore-fluid pressures as well as of stress and strain. Increases in pore-fluid pressure or injected fluid volume are assumed to cause ground-surface uplift that can be inferred from geodetic observations, such as Global Positioning System (GPS) and InSAR. These geodetic observations have been used to infer spatiotemporal ground surface uplift in regions with induced seismicity (e.g., Barnhart et al., 2014; Jiang et al., 2020) and surface deformation in geothermal regions (e.g., Fialko & Simons, 2000; Heimlich et al., 2015; Mossop & Segall, 1997).

Incorporating InSAR observations in studies investigating fluid injection induced seismicity was well demonstrated by Shirzaei et al. (2016, 2019) who applied a multitemporal InSAR approach to infer surface uplift due to wastewater disposal in eastern Texas, USA, where oil and gas developments, wastewater disposal, and induced seismicity occurred frequently (e.g., Frohlich, 2012; Frohlich & Brunt, 2013; Frohlich et al., 2014). The InSAR data were used to constrain surface and volumetric deformation, caused by subsurface pore-fluid pressure increases, due to subsurface fluid injection. They used three overlapping InSAR datasets for the Timpson area between 6 May 2007 and 14 November 2010 and determined a ground uplift rate of up to 3 mm yr⁻¹. Through inverse modeling, using the uplift rate, they estimated volumetric strain rates in the top 5 km of the crust and a total volume change rate of 800,000–1,000,000 m³ yr⁻¹, comparable to the reported volumetric rate of subsurface fluid injection.

Barnhart et al. (2014) demonstrated the utility of InSAR observations for monitoring and assessing fluid injection induced deformation. They used InSAR observations from 2011 around the 2011 M_w 5.3 Trinidad earthquake epicenter in the Raton Basin to constrain the rupture length to 8–10 km along a normal fault at a depth of 1.5–6.0 km in the basement. Wastewater disposal into the sedimentary rock above the basement was active at the time. While not always discerning a causal link between subsurface fluid injection and seismicity, InSAR applications help constrain spatial deformation associated with poroelastic deformation, benefitting studies of induced seismicity.

3.7. CO₂ Injection Success

As CO₂ injection is relevant to geoenergy development, we discuss in the following a few issues related to CO₂ injection induced seismicity. We acknowledge that we do not intend to offer a comprehensive review on CO₂ injection. Multiphase fluid geomechanics involved in CO₂ movement also requires different mathematical treatment than what is presented in the preceding sections of this paper.

3.7.1. Debate on Seismic Hazard From CO₂ Injection

Geologic carbon dioxide (CO₂) sequestration operations inject relatively large amounts of liquid CO₂ underground and yet have caused little seismicity. For example, at Sleipner in the North Sea, 1 million tonnes per year, or $\sim 5.6 \times 10^8$ m³ yr⁻¹, of CO₂ have been injected since 1996 into the Utsira formation (Halland et al., 2013; Lindeberg et al., 2009). For over 15 yr of this operation, the longest CO₂ sequestration project, no seismicity has been triggered (Zoback & Gorelick, 2012). In comparison, the largest cumulative volume injected at a wastewater disposal site, where induced seismicity has been studied, is 1.2×10^7 m³ (McGarr & Barbour, 2017; Yeck et al., 2017) at Prague, OK, USA.

Alarmed by the proliferation of induced seismicity from wastewater injection, Zoback and Gorelick (2012) warned that there is a high probability that earthquakes can be induced by the injection of CO₂, because of the large volumes of CO₂ that need to be sequestered worldwide to help reduce global climate change. They estimated that to contribute significantly to greenhouse gas emission reductions, roughly 3,500 sites, similar to the Sleipner site, are needed. They argued that preexisting faults in brittle rocks near (typically below) CO₂ storage reservoirs and common in continental interiors, respond to very small increases in pore-fluid pressure. They thus cautioned that even small-to moderate-sized earthquakes (in the basement rocks below the CO₂ storage formation), with centimeters of slip, could create permeable pathways and threaten the integrity of repository seals (caprocks) above the reservoir formations. They advocated to select CO₂ storage formations that are weakly cemented, porous, permeable, and laterally extensive to accommodate the injection of large volumes of CO₂ that only minimally increase pore-fluid pressures, so that CO₂ can be safely stored. Furthermore, they posed the question “whether the capacity exists for sufficient volumes of CO₂ to be stored geologically for it to have the desired beneficial effect on climate change” (Zoback & Gorelick, 2012, 2015).

In contrast, Vilarrasa and Carrera (2015) suggested that induced earthquakes, caused by geologic CO₂ storage, are unlikely to occur, based on the following argumentation:

1. CO₂ storage occurs typically in sedimentary formations that are softer than crystalline basement rocks and rarely as critically stressed as crystalline rocks. Zoback and Gorelick (2015) argued that the stress magnitudes in some sedimentary rocks are similar to those in crystalline rocks.
2. The evolution of pore-fluid overpressure from CO₂ injection significantly differs from that of wastewater injection, where overpressures could become large over very long injection intervals. The low viscosity of CO₂ implies that pore-fluid overpressures from CO₂ injection peak at the beginning of CO₂ injection and drops over time. Thus, the least mechanically stable situation is anticipated to occur at the beginning of CO₂ injection, which makes it much easier to control. Furthermore, through time, CO₂ dissolution into formation brines helps reduce overpressures (Kong & Saar, 2013). Zoback and Gorelick (2015), however, consider such CO₂ dissolution to be too small to make a difference in reducing overpressure.
3. Similarly, reducing the CO₂ storage reservoir's temperature, by conducting CO₂-Plume Geothermal (CPG) based energy extraction (Adams et al., 2021) would serve to reduce reservoir overpressures. To note, the amount of CO₂ stored is not reduced by CPG operations, as the produced CO₂ is reinjected into the CO₂ storage reservoir once the heat has been removed. However, water produced with the CO₂ would indeed be removed during CPG and related, such as CPG-based energy storage, operations (Buscheck et al., 2016; Fleming et al., 2020; Garapati et al., 2015), which would also serve to help reduce reservoir overpressures.
4. CO₂ does not easily transverse caprocks because of capillarity, while formation brines do, which reduces the overpressure in the CO₂ storage formation. Capillary entry pressures increase with both clay content and reduced pore size, which is what ultimately hinders CO₂ penetration into the fault.

No evidence exists from existing CO₂ storage projects that CO₂ has the potential to easily induce large earthquakes. Vilarrasa et al. (2019) reviewed potential mechanisms for inducing seismicity with CO₂ injection and called attention to three considerations that favor reducing seismicity occurrences, namely the use of not critically stressed sedimentary formations, identifying faults that are critically oriented for shear slip, monitoring and managing overpressures and seismicity.

These spirited discussions and insights are illuminating regarding the geomechanics and multiphase fluid dynamics at CO₂ sequestration sites. One consensus coming out of these discussions appears to be that properly sited and managed, CO₂ storage in deep saline formations remains a viable option for mitigating anthropogenic climate change effects through subsurface CO₂ storage. While the limited capacity for CO₂ storage remains a concern, some CO₂ storage in depleted gas fields have proven to be safe, where infrastructures exist, rock properties have been characterized, and formation pressures are low (e.g., Jenkins et al., 2012; Prinet et al., 2013).

3.7.2. Favorable Conditions Minimizing Seismicity

Verdon et al. (2013) compared the geomechanical conditions of three significant commercial carbon capture and storage (CCS) sites, with CO₂ injection rates of ~1 Mt yr⁻¹, namely the Sleipner Field in the Norwegian North Sea, the Weyburn Field in central Canada, and the In Salah Field in Algeria. The study addressed concerns of geomechanical deformation creating, or reactivating, fractures and faults in the sealing caprocks, potentially causing CO₂ leakage. Such a comparison can be informative to examine the geomechanical conditions related to induce seismicity.

At Sleipner, a significant amount of CO₂ is coproduced with natural gas and ~1 million tonnes of CO₂ have been injected per year into the Utsira formation (Halland et al., 2013; Lindeberg et al., 2009) since 1996. The Utsira formation is a laterally extensive and vertically isolated saline aquifer. It consists of poorly cemented sandstones that are porous and permeable. The formation deforms slowly, so that stresses relax over time. It is considered an excellent reservoir (Halland et al., 2013). A total of 18×10^6 m³ CO₂ have been injected by 2011, but the available pore volume is estimated at 6×10^{11} m³, which is orders of magnitude greater than the injected CO₂ volume (Chadwick et al., 2012). The permeable reservoir condition and a large pore volume available for CO₂ storage led to little pore-fluid pressure changes due to the CO₂ injection, which appears to be the key factor for not inducing seismicity.

The Weyburn oilfield in Canada has been producing oil for over 50 yr and CO₂ has been injected into the field since 2000 to enhance oil recovery and to permanently store some of the injected CO₂ (Verdon et al., 2013). The Weyburn reservoir is a 30–40 m thick dolostone and limestone at a depth of a ~1,430 m. About 3 Mt of CO₂ are injected per year. On-site seismic monitoring detected only microseismicity that was primarily occurring near the

production wells, rather than the injection wells, as well as in the overburden. The history of fluid injection, pore-fluid pressure, and seismicity does not seem to show clear correlations. This puzzling phenomenon, and concerns over the future safety of the CO₂ storage site, motivated a poroelasticity, geomechanical modeling study (Verdon et al., 2011). Microseismicity locations were used as a constraint for the model-predicted geomechanical state. Using mechanical properties, much softer than values measured on rock core samples, the model predicted that mechanical failures were more consistent with observed microseismicity locations than predictions using values from rock core measurements. The softer mechanical properties and deformation in the reservoir transferred stresses to the overburden and caused shear stress changes there. Near the fluid injection well, both normal and shear stresses were reduced, however, shear stress reductions were larger than normal stress reductions. Thus, no seismicity was caused. While the microseismicity is indicative of mechanical conditions triggering failures of small fractures, it is reasonable to extrapolate that larger seismic events could have happened if larger critically stressed faults had been present at the site (Verdon et al., 2013). Thus, the absence of faults is perhaps a key factor for a lack of induced seismicity at Weyburn.

The In Salah CCS facility in central Algeria captured CO₂ from several gas fields that contains 5%–10% CO₂ (Verdon et al., 2015). CO₂ is then compressed and injected into the 20 m thick Carboniferous sandstone formation at 1.9 km depth. The reservoir is overlain by a seal of 950 m of mudstones. Over 3.8 million tonnes of CO₂ were injected to the subsurface between 2004 and 2011 (Ringrose et al., 2013; Verdon et al., 2015). Seismicity, CO₂ gas tracers, logging and core analyses, groundwater monitoring, InSAR, as well as geochemical and rock mechanics modeling were used to assess the performance of the project and identify risks associated with the operation. CO₂ plume migration, well integrity, and leakage into caprock were the major risks identified (Ringrose et al., 2013). Fluid injection caused high pore-fluid overpressures and rock deformation (Bissell et al., 2011), and fracture networks were revealed by InSAR-observed surface uplift (Onuma & Ohkawa, 2009; Vasco et al., 2010). CO₂ leakage into the caprock also became a concern. Consequently, CO₂ injection was suspended in 2011 to alleviate pore-fluid overpressures. Seismicity monitoring located ~3,600–6,300 events with magnitudes of up to 1.7 (Goertz-Allmann et al., 2014; Stork et al., 2015). These events followed a Gutenberg-Richter distribution with an elevated *b* value of 2.17 ± 0.09 , which is characteristic of fluid-injection induced seismicity (Verdon et al., 2015). Geomechanical modeling predicted fluid injection induced seismic events closely matching the largest event observed at In Salah and suggested that geomechanical deformation can pose a risk to CCS projects by compromising the integrity of the caprock and by triggering seismicity (Verdon et al., 2015). As the earthquake magnitudes were small and infrastructures at the land surface are sparse, the overall seismicity risk has been small.

3.7.3. Little Seismicity Hazard at Emerging CO₂ Storage Sites

There are numerous newer and smaller CO₂ storage operations that have not observed induced seismicity. For example, the Aquistore CCS project in Saskatchewan, Canada, where, to the date of this writing (2021), about 350,000 t of CO₂ have been injected since 2015 into a basal Cambrian sandstone at a depth of about 3.4 km and no induced seismicity has been observed (Stork et al., 2018). The analysis conducted by Stork et al. (2018) was on the data collected during the early days of the project when only ~140,000 t of CO₂ were injected and the injection pressure was below the fracturing pressure. They advocated for continued seismic monitoring to provide warning of potential increases in seismicity and pressures near faults. Similarly, the Quest CCS facility in Alberta, Canada, has captured and safely stored 4 million tonnes of CO₂ from 2015 to 2019, where only microseismicity of magnitude <0 has been observed, showing little seismic risk (O'Brien et al., 2018).

The Decatur ethanol plant in Illinois, USA, began to inject 1 million tonnes of CO₂ per year in 2017 (Yang et al., 2018). The injection occurred in the Cambrian Mt. Simon Sandstone in the Illinois Basin that underlies a large part of Illinois and part of Indiana and Kentucky. The Mt. Simon Sandstone, at a depth of 1,690–2,184 m, with a gross thickness of 494 m, is relatively porous and permeable, with horizontal permeability ranging from $\sim 10^{-18}$ to 10^{-14} m² (Frailey et al., 2011). The Mt. Simon Sandstone has great potential as a reservoir for storing CO₂ and multiple projects are exploring CCS in this formation. Numerical modeling of CO₂ plumes from multiple sites suggest that operation can be designed so that the plumes will have no contact (Yang et al., 2018). Therefore, the site may open a door for multiple users to commercialize CO₂ storage.

Kaven et al. (2015) conducted an in-depth seismicity study and found that no seismicity greater than $M_w 1.26$ has been observed at Decatur after ~1 million tonnes of supercritical CO₂ had been injected. They further suggest

that the microseismicity that did occur at Decatur is unlikely a hazard to the seal integrity of the overlying caprock. However, they cautioned that the low-magnitude seismicity at the Decatur site shares similar characteristics to the larger-magnitude injection-induced seismicity elsewhere (e.g., Kim, 2013) and called for more research to understand the impact of long-term CO₂ injection and induced seismicity at the CCS site.

While most CCS operations did not induce felt earthquakes, Gan and Frohlich (2013) did find 18 earthquakes with magnitude 3 and greater in the Cogdell oil field in Texas between 2006 and 2011, which may have been caused by the injection of significant volumes of fluids since 2004, including that of supercritical CO₂. They suggest that further modeling studies, that consider not only seismology but also hydrogeology and geomechanics, are needed to evaluate the assertion that significant risks accompany large-scale CCS as a strategy for mitigating climate change.

4. Conclusions

While many studies have been conducted that focus on one particular mechanism for a specific earthquake sequence, an increasing number of studies explore the potential of multiple processes triggering earthquakes. Our review here also suggests that commonly multiple processes operate in concert, sequentially or contemporaneously, in inducing seismicity. Not intended to be exhaustive, Table 1 lists some relevant examples with their respective triggering mechanisms.

Table 1
List of Injection Induced Seismicity Examples With their Respective Triggering Mechanisms

Operation	Location	Maximum magnitude	Year	Triggering mechanisms	Representative references
Hydraulic fracturing and EGS	Basel, Switzerland	M _L 3.4	2016	Pore-fluid pressure diffusion	Mukuhira et al., 2017
Hydraulic fracturing and EGS	Pohang, Korea	M _w 5.5	2017	Pore-fluid pressure diffusion, Coulomb static stress, and poroelasticity	Yeo et al., 2020 Chang et al., 2020
Hydraulic fracturing and EGS	Soultz-sous-Forêts, France	M2.9	2003	Pore-fluid pressure diffusion	Charlétty et al., 2007 Baisch et al., 2010
Hydraulic fracturing and natural geothermal system	Brawley, CA, USA	M _w 5.4	2012	Aseismic slip	Wei et al., 2015
Hydraulic fracturing and oil/gas	Fox Creek, AB, Canada	M _w 4.1	2016	Pore-fluid pressure diffusion and poroelasticity	Schultz et al., 2017 Shen et al., 2019 Hui et al., 2021
Hydraulic fracturing and oil/gas	Horn River, AB, Canada	M _L 3.6	2011		Farahbod et al., 2015
Hydraulic fracturing and oil/gas	Blackpool, UK	M _L 2.3	2011		Clarke et al., 2014
Wastewater disposal	Denver, USA	M4.4	1963	Pore-fluid pressure diffusion	Hsieh & Bredehoeft, 1981
Wastewater disposal	Fairview, OK, USA	M _w 5.1	2016	Pore-fluid pressure diffusion and poroelasticity	Goebel et al., 2017
Wastewater disposal	Pawnee, OK, USA	M _w 5.8	2016	Pore-fluid pressure diffusion, poroelasticity, and Coulomb static stress	Barbour et al., 2017 Chen et al., 2017
Wastewater disposal	Cushing, OK, USA	M _w 5.0	2016	Pore-fluid pressure diffusion and poroelasticity	Zhai et al., 2019 Deng et al., 2020
Wastewater disposal	Prague, OK, USA	M5.7	2011	Coulomb static stress	Sumy et al., 2014
Wastewater disposal	Raton, CO, USA	M5.3	2011	Pore-fluid pressure diffusion	Nakai et al., 2017
Wastewater disposal	Timpson, TX, USA	M _w 4.8	2012	Pore-fluid pressure diffusion and poroelasticity	Shirzaei et al., 2016
Wastewater disposal	Delaware Basin, TX, USA	M5	2020	Pore-pressure diffusion	Tung et al., 2021
In situ experiments	France			Aseismic slip	Guglielmi et al., 2015
Lab experiment				Pore-fluid pressure diffusion and poroelasticity	Alghannam & Juanes, 2020
Generic study				Pore-fluid pressure diffusion and poroelasticity	Segall & Lu, 2015
Generic study				Pore-fluid pressure diffusion and Coulomb static stress	Brown & Ge, 2018b

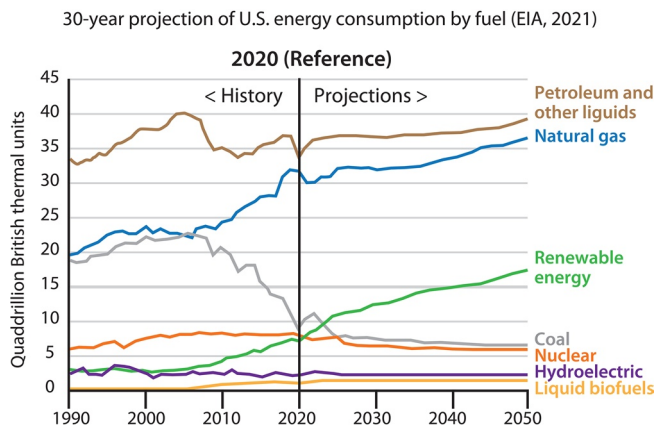


Figure 11. Projection of US energy consumption by fuel for the next 30 yr (after EIA, 2021).

We draw the following conclusions from this review.

1. Pore-fluid pressure diffusion remains a fundamental mechanism for inducing seismicity. It cross-cuts nearly all case studies and plays an important role, particularly in inducing near-field and early time seismicity. We note that here pore-fluid pressure dominance in the near field is primarily based on the notion that pore-fluid pressure is the largest near injection and often has a greater effect on the Coulomb stress on a fault than the effects of poroelastic stresses have.
2. Poroelastic stresses are increasingly recognized to contribute to stress changes on faults, causing fault slip. Compared to pore-fluid pressure changes from diffusion, poroelastic stress changes are usually small near subsurface fluid injection locations but can become significant in the far-field, beyond the spatial influence of pore-fluid pressure diffusion. Poroelasticity stress changes, along with pore-pressure diffusion and aseismic slip, have been identified to cause far-field stress changes. There are no cases, where far-field seismicity can be attributed exclusively to poroelastic stress changes.
3. Coulomb static stress transfer has also been shown to be a viable mechanism for increasing the stresses on mainshock faults, primarily from earlier seismicity in a sequence including major foreshocks
4. Multiple mechanisms have operated concurrently or sequentially at most induced seismicity sites. For example, poroelastic stresses and Coulomb static stress transfer are invoked to explain post-fluid injection earthquakes.
5. CO₂ injection appears to be succeeding without inducing earthquakes. There is much to be learned from its success. Lacking critically stressed faults and limited pore-fluid pressure buildup are recognized factors attributing to not inducing seismicity at CCS sites.

5. Future Research Opportunities

Case studies reviewed in this article and in the literature suggest that studying induced seismicity often requires integrating knowledge from seismology, hydrogeology, geomechanics, and thermodynamics. As direct in situ observations at depths below a few kilometers, such as pore-fluid pressure and stress or strain, are rare, study approaches have embraced indirect inferences of numerical modeling exercises and of remote sensing data. Advances are being made along both fronts. In the meantime, these advances also bring out new research opportunities to a broader community of earth scientists. The following provides some research examples and scientific questions that, in our minds, deserve attention (Figure 11).

1. Efforts to quantify the geomechanical state of areas of interest, including stresses and pore-fluid pressure, are much needed, as the stresses on faults ultimately control whether, where, and when faults slip. As an example, Shen et al. (2021) demonstrate a recent effort toward addressing this need. On the basis of geophysical logs and field testing in the West Shale Basin in Canada, they developed a quantitative 3D stress distribution model for determining the maximum and minimum horizontal stress, vertical stress, stress orientation, as well as ambient pore pressure. These variables are then used to evaluate the mechanical stability of the faults in the area of interest (Snee & Zoback, 2018; Zhang et al., 2021).
2. Seismic hazard forecasts rely on the assessment of historical natural earthquakes and probabilities of earthquake magnitudes, frequency, location, as well as ground mechanical properties (Cornell, 1968). As damages from induced seismicity became apparent in the recent decade, short-term induced seismicity began to be incorporated into seismic hazard studies (e.g., Ghofrani et al., 2019; Petersen et al., 2016; Rubinstein et al., 2021). Using the stress rate from hydromechanical models and a rate-and-state model to simulate seismicity rate changes through time, Zhai et al. (2020) added new physical insights to seismic hazard forecasting involving long-term background earthquakes and time-varying induced earthquakes. More research is called for to better understand induced earthquakes from wastewater injection and fracking operations (Petersen et al., 2018) and further integration and implementation of physics-based models into seismic hazard studies, translating scientific knowledge into practice of effective mitigating strategies.

3. What are the potential impacts of fluid injection on the natural hydrologic cycle when a large amount of fluid is added to the subsurface? Projection for energy use in the coming decades (Figure 11) point to a continued dominance of oil and natural gas, but also show a growing trajectory for renewable energy use that includes geothermal (EIA, 2021). Consequently, the demand for water to enhance the production of oil, gas, and geothermal energy production from the subsurface and the need for underground wastewater disposal will only intensify. The potential impact of intensified water extraction and injection on the water cycle in the shallow crust has yet to be examined
4. What are the geochemical implications of subsurface fluid injection, that is, how may the water quality around fluid injection sites change over time. A related question concerns potential mineral precipitation or dissolution reactions and how they may alter the required high permeability of injection formations with implications for the native fluid flow field as well as the ability to continue fluid injection/extraction (Luhmann et al., 2014, 2017; Tutolo et al., 2014). Furthermore, the density contrast between injected wastewater and formation fluid is often high enough to create a gravitational drive for the injected water to sink deeper (Pollyea et al., 2019), a suggested reason for causing seismicity occurring at later times below the fluid injection location. Geochemical implications of injecting these dense wastewaters are much less understood.
5. The significant increase in data availability over the past decades has promoted a robust increase in studies that correlate spatially and temporally subsurface fluid injection and seismicity occurrences (Pollyea et al., 2018; Weingarten et al., 2015). Furthermore, mining such fluid injection data to potentially develop a comprehensive database could better illuminate spatiotemporal relations among seismicity, hydrogeological, and mechanical properties of rock formations and of operational fluid injection parameters. Such databases can also complement and help constrain process-based modeling studies.
6. Current modeling efforts, numerical or analytical, appear to largely depend on the involved researchers' familiarity with, and availability of, or access to, various numerical simulators. Fully coupled, multi-process (i.e., thermal (T), hydraulic (H), mechanical (M), chemical (C), THMC) modeling studies remain rare, even though subsets of numerical THMC studies exist such as reactive transport studies, representing (T)HC modeling (e.g., Leal et al., 2017; Tutolo et al., 2015, 2020). Examples of a HMC studies, with implications particularly for fluid injectivity and/or CO₂ storage mechanisms and thus induced seismicity, are Luhmann et al. (2013) and Ma et al. (2020). The latter study investigated mineral dissolution effects on the effective stress law for permeability. Yet, the desire for fully coupled models lingers and arguments have been made that a full integration of various processes is necessary to better understand induced seismicity hazard (e.g., Zhai et al., 2020). A sophisticated poroelastic numerical model was developed by Jin and Zoback (2017) to examine coupled nonlinear pore-pressure diffusion and poroelastic deformation in arbitrarily fractured porous media. We believe that a holistic assessment of modeling approaches to study induced seismicity is called for to examine what processes can and cannot be ignored and to compare the strengths and weaknesses of various modeling approaches.
7. There is a need for in situ and laboratory characterization of mechanical and hydrological properties of rocks and faults. Modeling studies heavily depend on those material properties as input, yet, most have used inferred or proxy data based on similar rock types. Efforts along this line have proven valuable. For example, Scuderi et al. (2020) tested frictional rock properties on samples made of in-situ collected rocks. Their laboratory experiment results showed that slow slip events represent frictional instabilities determined by local boundary conditions and their observed events agree with the slow slip observed in some natural tectonic environments, thereby providing mechanical constraints to help establish links between the observed induced seismicity and laboratory-derived theoretical fault mechanics.
8. Geodetic observations such as InSAR have shown promise when inferring subsurface processes from ground surface deformation. Given that direct monitoring data of the subsurface, such as pore-fluid pressure or rock deformation, are rare, geodetic observations may fill-in at least in part the data needed to calibrate models. Advances are needed to utilize these observations to constrain the poroelastic deformation as well as to infer mechanical and hydrogeologic properties of the subsurface.

Data Availability Statement

Data were not used or created for this article. The authors greatly appreciate the comments provided by Editor Douglas Schmit, Associate Editor, Pathikrit Bhattacharya, and two anonymous reviewers. The comments helped to significantly enhance the quality of the article.

Acknowledgments

Shemin Ge acknowledges partial support from the United States Department of Energy Grant (DE-SC0020222), a Fulbright US Scholar Fellowship, and a visiting professorship in the Earth Sciences Department at ETH Zurich, Switzerland. Martin O. Saar acknowledges partial support of the Geothermal Energy and Geofluids (GEG.ethz.ch) group at ETH Zurich, Switzerland, by the Werner Siemens Foundation (Werner Siemens-Stiftung).

References

- Adams, B. M., Vogler, D., Kuehn, T. H., Bielicki, J. M., Garapati, N., and Saar, M. O. (2021). Heat depletion in sedimentary basins and its effect on the design and electric power output of CO₂ plume geothermal (CPG) systems. *Renewable Energy*, *172*, 1393–1403. <https://doi.org/10.1016/j.renene.2020.11.145>
- Alghannam, M., & Juanes, R. (2020). Understanding rate effects in injection-induced earthquakes. *Nature Communications*, *11*, 3053. <https://doi.org/10.1038/s41467-020-16860-y>
- Altmann, J. B., Müller, B. I. R., Müller, T. M., Heidbach, O., Tingay, M. R. P., & Weißhardt, A. (2014). Pore pressure stress coupling in 3D and consequences for reservoir stress states and fault reactivation. *Geothermics*, *52*, 195–205. <https://doi.org/10.1016/j.geothermics.2014.01.004>
- Amann, F., Gischig, V., Evans, K., Doetsch, J., Jalali, R., Valley, B., et al. (2018). The seismo-hydro-mechanical behaviour during deep geothermal reservoir stimulations: Open questions tackled in a decameter-scale in-situ stimulation experiment. *Solid Earth*, *9*, 115–137. <https://doi.org/10.5194/se-9-115-2018>
- Atkinson, G. M., Eaton, D. W., Ghofrani, H., Walker, D., Cheadle, B., Schultz, R., et al. (2016). Hydraulic fracturing and seismicity in the western Canada sedimentary basin. *Seismological Research Letters*, *87*, 631–647. <https://doi.org/10.1785/0220150263>
- Atkinson, G. M., Eaton, D. W., & Igonin, N. (2020). Developments in understanding seismicity triggered by hydraulic fracturing. *Nature Reviews Earth & Environment*, *1*, 264–277. <https://doi.org/10.1038/s43017-020-0049-7>
- Baisch, S., Vörös, R., Rothert, E., Stang, H., Jung, R., & Schellschmidt, R. (2010). A numerical model for fluid injection induced seismicity at Soultz-sous-Forêts. *International Journal of Rock Mechanics and Mining Sciences*, *47*(3), 405–413. <https://doi.org/10.1016/j.ijrms.2009.10.001>
- Ball, L., Ge, S., Caine, J. S., Revil, A., & Jardani, A. (2010). Constraining fault-zone hydrogeology through integrated hydrological and geoelectrical analysis. *Hydrogeology Journal*, *18*. <https://doi.org/10.1007/s10040-010-0587-z>
- Bao, X., & Eaton, D. W. (2016). Fault activation by hydraulic fracturing in western Canada. *Science*, *354*(6318), 1406–1409. <https://doi.org/10.1126/science.aag2583>
- Baranova, V., Mustaqeem, A., & Bell, S. (1999). A model for induced seismicity caused by hydrocarbon production in the Western Canada Sedimentary Basin. *Canadian Journal of Earth Sciences*, *36*(1), 47–64. <https://doi.org/10.1139/e98-080>
- Barbour, A. J., Norbeck, J. H., & Rubinstein, J. L. (2017). The effects of varying injection rates in Osage county, Oklahoma, on the 2016 M_w 5.8 Pawnee earthquake. *Seismological Research Letters*, *88*(4), 1–14. <https://doi.org/10.1785/0220170003>
- Barenblatt, G. I., Zheltov, I. P., & Kocina, I. N. (1960). Basic concepts in the theory of seepage of homogeneous liquids in fissured rocks (strata). *Journal of Applied Mathematics and Mechanics*, *24*(5), 1286–1303. [https://doi.org/10.1016/0021-8928\(60\)90107-6](https://doi.org/10.1016/0021-8928(60)90107-6)
- Barnhart, W. D., Benz, H. M., Hayes, G. P., Rubinstein, J. L., & Bergman, E. (2014). Seismological and geodetic constraints on the 2011 Mw 5.3 Trinidad, Colorado earthquake and induced deformation in the Raton Basin. *Journal of Geophysical Research*, *119*(10), 7923–7933. <https://doi.org/10.1002/2014JB011227>
- Barton, C. A., Zoback, M. D., & Moos, D. (1995). Fluid flow along potentially active faults in crystalline rock. *Geology*, *23*(8), 683–686. [https://doi.org/10.1130/0091-7613\(1995\)023<0683:FFAPAF>2.3.CO;2](https://doi.org/10.1130/0091-7613(1995)023<0683:FFAPAF>2.3.CO;2)
- Bhattacharya, P., & Viesca, R. C. (2019). Fluid-induced aseismic fault slip outpaces pore-fluid migration. *Science*, *364*(6439), 464–468. <https://doi.org/10.1126/science.aaw7354>
- Biot, M. A. (1941). General theory of 3-dimensional consolidation. *Journal of Applied Physics*, *12*, 155–164. <https://doi.org/10.1063/1.1712886>
- Bissel, R. C., Vasco, D. W., Atbi, M., Hamdani, M., Okwelegbe, M., & Goldwater, M. H. (2011). A full field simulation of the in Salah gas production and CO₂ storage project using a coupled geo-mechanical and thermal fluid flow simulator. *Energy Procedia*, *4*, 3290–3297. <https://doi.org/10.1016/j.egypro.2011.02.249>
- Bommer, J. J., Oates, S., Cepeda, J. M., Lindholm, C., Bird, J., Torres, R., et al. (2006). Control of hazard due to seismicity induced by a hot fractured rock geothermal project. *Engineering Geology*, *83*, 287–306. <https://doi.org/10.1016/j.enggeo.2005.11.002>
- Bourouis, S., & Bernard, P. (2007). Evidence for coupled seismic and aseismic fault slip during water injection in the geothermal site of Soultz (France), and implications for seismogenic transients. *Geophysical Journal International*, *169*(2), 723–732. <https://doi.org/10.1111/j.1365-246X.2006.03325.x>
- Bredehoeft, J. D., Belitz, K., & Sharp-Hansen, S. (1992). The hydrodynamics of the Big Horn Basin: A study of the role of faults. *The American Association of Petroleum Geologists Bulletin*, *76*, 530–546. <https://doi.org/10.1306/BDF8862-1718-11D7-8645000102C1865D>
- Breede, K., Dzebisashvili, K., Liu, X., & Falcone, G. (2013). A systematic review of enhanced (or engineered) geothermal systems: Past, present and future. *Geothermal Energy*, *1*, 4. <https://doi.org/10.1186/2195-9706-1-4>
- Brown, M. R., & Ge, S. (2018a). Distinguishing fluid flow path from pore pressure diffusion for induced seismicity. *Bulletin of the Seismological Society of America*, *108*(6), 3684–3686. <https://doi.org/10.1785/0120180149>
- Brown, M. R., & Ge, S. (2018b). Small earthquakes matter in injection induced seismicity. *Geophysical Research Letters*, *45*. <https://doi.org/10.1029/2018GL077472>
- Buscheck, T. A., Bielicki, J. M., Edmunds, T. A., Hao, Y., Sun, Y., Randolph, J. B., & Saar, M. O. (2016). Multifluid geo-energy systems: Using geologic CO₂ storage for geothermal energy production and grid-scale energy storage in sedimentary basins. *Geosphere*, *12*(3), 678–696. <https://doi.org/10.1130/GES01207.1>
- Caine, J. S., Evans, J. P., & Forster, C. B. (1996). Fault zone architecture and permeability structure. *Geology*, *24*, 1025–1028. [https://doi.org/10.1130/0091-7613\(1996\)024<1025:FZAAAPS>2.3.CO;2](https://doi.org/10.1130/0091-7613(1996)024<1025:FZAAAPS>2.3.CO;2)
- Cardiff, M., Lim, D. D., Patterson, J. R., Akerley, J., Spielman, P., Lopeman, J., et al. (2018). Geothermal production and reduced seismicity: Correlation and proposed mechanism. *Earth and Planetary Science Letters*, *482*, 470–477. <https://doi.org/10.1016/j.epsl.2017.11.037>
- Carslaw, H. S. (1921). *Introduction to the mathematical theory of the conduction of heat in solids* (2nd ed., p. 152). Macmillan.
- Carslaw, H. S., & Jaeger, J. C. (1959). *Conduction of heat in solids* (p. 517). Oxford University Press.

- Chadwick, R. A., Williams, G. A., Williams, J. D. O., & Noy, D. J. (2012). Measuring pressure performance of a large saline aquifer during industrial-scale CO₂ injection: The Utsira Sand, Norwegian North Sea. *International Journal of Greenhouse Gas Control*, *10*, 374–388. <https://doi.org/10.1016/j.ijggc.2012.06.022>
- Chang, K. W., & Segall, P. (2016). Injection-induced seismicity on basement faults including poroelastic stressing. *Journal of Geophysical Research*, *121*, 2708–2726. <https://doi.org/10.1002/2015JB012561>
- Chang, K. W., Yoon, H., Kim, Y. H., & Lee, M. Y. (2020). Operational and geological controls of coupled poroelastic stressing and pore-pressure accumulation along faults: Induced earthquakes in Pohang, South Korea. *Scientific Reports*, *10*, 2073. <https://doi.org/10.1038/s41598-020-58881-z>
- Charl y, J., Cuenot, N., Dorbath, L., Dorbath, C., Haessler, H., & Frogneux, M. (2007). Large earthquakes during hydraulic stimulations at the geothermal site of Soultz-sous-For ts. *International Journal of Rock Mechanics and Mining Sciences*, *44*, 1091–1105. <https://doi.org/10.1016/j.ijrmms.2007.06.003>
- Chen, X., Nakata, N., Pennington, C., Haffener, J., Chang, J. C., He, X., et al. (2017). The Pawnee earthquake as a result of the interplay among injection, faults and foreshocks. *Scientific Reports*, *7*, 4945. <https://doi.org/10.1038/s41598-017-04992-z>
- Christiansen, L. B., Hurwitz, S., Saar, M. O., Ingebritsen, S. E., & Hsieh, P. A. (2005). Seasonal seismicity at western United States volcanic centers. *Earth and Planetary Science Letters*, *240*, 307–321. <https://doi.org/10.1016/j.epsl.2005.09.012>
- Clark, J. B. (1949). A hydraulic process for increasing the productivity of wells. *Journal of Petroleum Technology*, *186*, 1–8. <https://doi.org/10.2118/949001-G>
- Clarke, H., Eisner, L., Styles, P., & Turner, P. (2014). Felt seismicity associated with shale gas hydraulic fracturing: The first documented example in Europe. *Geophysical Research Letters*, *41*, 8308–8314. <https://doi.org/10.1002/2014GL062047>
- Cleary, M. P. (1977). Fundamental solutions for a fluid-saturated porous solid. *International Journal of Solids and Structures*, *13*, 785–806. [https://doi.org/10.1016/0020-7683\(77\)90065-8](https://doi.org/10.1016/0020-7683(77)90065-8)
- Cocco, M., & Rice, J. R. (2002). Pore pressure and poroelasticity effects in Coulomb stress analysis of earthquake interactions. *Journal of Geophysical Research*, *107*(B2). <https://doi.org/10.1029/2000JB000138>
- Cochran, E. S., Ross, Z. E., Harrington, R. M., Dougherty, S. L., & Rubinstein, J. L. (2018). Induced earthquake families reveal distinctive evolutionary patterns near disposal wells. *Journal of Geophysical Research*, *123*(9), 8045–8055. <https://doi.org/10.1029/2018JB016270>
- COMSOL. (2018). *COMSOL multiphysics manual version 5* (Vol. 4).
- Cornell, C. A. (1968). Engineering seismic risk analysis. *Bulletin of the Seismological Society of America*, *58*, 1583–1606. <https://doi.org/10.1785/BSSA0580051583>
- Cornet, F. H. (2016). Seismic and aseismic motions generated by fluid injections. *Geomechanics for Energy and the Environment*, *5*, 42–54. <https://doi.org/10.1016/j.gete.2015.12.003>
- Cornet, F. H., Helm, J., Poitrenaud, H., & Etchecopar, A. (1997). Seismic and aseismic slips induced by large-scale fluid injections. *Pure and Applied Geophysics*, *150*, 563–583. <https://doi.org/10.1007/s000240050093>
- Davis, S. D., & Frohlich, C. (1993). Did (or will) fluid injection cause earthquakes?—Criteria for a rational assessment. *Seismological Research Letters*, *64*, 207–224. <https://doi.org/10.1785/gssrl.64.3-4.207>
- Deichmann, N., & Giardini, D. (2009). Earthquakes induced by the stimulation of an enhanced geothermal system below Basel (Switzerland). *Seismological Research Letters*, *80*(5), 784–798. <https://doi.org/10.1785/gssrl.80.5.784>
- Deng, K., Liu, Y., & Chen, X. (2020). Correlation between poroelastic stress perturbation and multidisposal wells induced earthquake sequence in Cushing, Oklahoma. *Geophysical Research Letters*, *47*, e2020GL089366. <https://doi.org/10.1029/2020GL089366>
- Detournay, E., & Cheng, A. H.-D. (1993). In C. Fairhurst (Ed.), *Fundamentals of poroelasticity. Chapter 5 in comprehensive rock engineering: Principles, practice and projects, analysis and design method* (Vol. II, pp. 113–171). Pergamon Press.
- Dieterich, J. (1994). A constitutive law for rate of earthquake production and its application to earthquake clustering. *Journal of Geophysical Research*, *99*(B2), 2601–2618. <https://doi.org/10.1029/93JB02581>
- Doan, M. L., Brodsky, E. E., Kano, Y., & Ma, K. F. (2006). In situ measurement of the hydraulic diffusivity of the active Chelungpu Fault, Taiwan. *Geophysical Research Letters*, *33*, L16317. <https://doi.org/10.1029/2006GL026889>
- Eaton, D. W., Igonin, N., Poulin, A., Weir, R., Zhang, H., Pellegrino, S., & Rodriguez, G. (2018). Induced seismicity characterization during hydraulic fracture monitoring with a shallow-wellbore geophone array and broadband sensors. *Seismological Research Letters*, *89*, 1641–1651. <https://doi.org/10.1785/0220180055>
- EIA (US Energy Information Administration). (2021). *Annual energy outlook 2021 with projections to 2050*. Retrieved from https://www.eia.gov/outlooks/aeo/pdf/AEO_Narrative_2021.pdf
- Ellsworth, W. L. (2013). Injection-induced earthquakes. *Science*, *341*. <https://doi.org/10.1126/science.1225942>
- Ellsworth, W. L., Giardini, D., Townend, J., Ge, S., & Shimamoto, T. (2019). Triggering of the Pohang, Korea, earthquake (Mw 5.5) by enhanced geothermal system stimulation. *Seismological Research Letters*, *90*(5), 1844–1858. <https://doi.org/10.1785/0220190102>
- Elsworth, D., Spiers, C. J., & Niemeijer, A. R. (2016). Understanding induced seismicity: Observational data sets provide a clearer picture of the causes of induced seismicity. *Science*, *354*(6318), 1380–1381. <https://doi.org/10.1126/science.aal2584>
- Evans, D. M. (1966). The Denver area earthquakes and the Rocky Mountain Arsenal disposal well. *The Mountain Geologist*, *3*(1), 23–36. <https://doi.org/10.1130/Eng-Case-8.25>
- Evans, K. F., Zappone, A., Kraft, T., Deichmann, N., & Moia, F. (2012). A survey of the induced seismic responses to fluid injection in geothermal and CO₂ reservoirs in Europe. *Geothermics*, *41*, 30–54. <https://doi.org/10.1016/j.geothermics.2011.08.002>
- Eyre, T. S., Eaton, D. W., Garagash, D. I., Zecevic, M., Venieri, M., Weir, R., & Lawton, D. C. (2019). The role of aseismic slip in hydraulic fracturing-induced seismicity. *Science Advances*, *5*, eaav7172. <https://doi.org/10.1126/sciadv.aav7172>
- Eyre, T. S., Eaton, D. W., Zecevic, M., D'Amico, D., & Kolos, D. (2019). Microseismicity reveals fault activation before Mw 4.1 hydraulic-fracturing induced earthquake. *Geophysical Research Letters*, *46*, 534–546. <https://doi.org/10.1029/2018GL079016>
- Fan, Z., Eichhubl, P., & Gale, J. F. W. (2016). Geomechanical analysis of fluid injection and seismic fault slip for the Mw4.8 Timpson, Texas, earthquake sequence. *Journal of Geophysical Research*, *121*, 2798–2812. <https://doi.org/10.1002/2016JB012821>
- Fan, Z., Eichhubl, P., & Newell, P. (2019). Basement fault reactivation by fluid injection into sedimentary reservoirs: Poroelastic effects. *Journal of Geophysical Research*, *124*, 7354–7369. <https://doi.org/10.1029/2018JB017062>
- Farahbod, A. M., Kao, H., Walker, D. M., & Cassidy, J. F. (2015). Investigation of regional seismicity before and after hydraulic fracturing in the Horn River Basin, northeast British Columbia. *Canadian Journal of Earth Sciences*, *52*(2), 112–122. <https://doi.org/10.1139/cjes-2014-0162>
- Fialko, Y., & Simons, M. (2000). Deformation and seismicity in the Coso geothermal area, Inyo County, California: Observations and modeling using satellite radar interferometry. *Journal of Geophysical Research*, *105*(B9), 2178–21793. <https://doi.org/10.1029/2000JB900169>
- Fleming, M. R., Adams, B. M., Kuehn, T. H., Bielicki, J. M., & Saar, M. O. (2020). Increased power generation due to exothermic water exsolution in CO₂ plume geothermal (CPG) power plants. *Geothermics*, *88*, 101865. <https://doi.org/10.1016/j.geothermics.2020.101865>

- Foulger, G. R., Wilson, M. P., Gluyas, J. G., Julian, B. R., & Davies, R. J. (2018). Global review of human-induced earthquakes. *Earth-Science Reviews*, 178, 438–514. <https://doi.org/10.1016/j.earscirev.2017.07.008>
- Frailey, S. M., Damico, J., & Leetaru, H. E. (2011). Reservoir characterization of the Mt. Simon sandstone, Illinois Basin, USA. *Energy Procedia*, 4, 5487–5494. <https://doi.org/10.1016/j.egypro.2011.02.534>
- Freeze, A. R., & Cherry, J. (1979). *Groundwater*. Prentice-Hall. Retrieved from <http://hydrogeologistswithoutborders.org/wordpress/1979-english/>
- Frohlich, C. (2012). Two-year survey comparing earthquake activity and injection-well locations in the Barnett Shale, Texas. *Proceedings of the National Academy of Sciences of the United States of America*, 109, 13934–13938. <https://doi.org/10.1073/pnas.1207728109>
- Frohlich, C., & Brunt, M. (2013). Two-year survey of earthquakes and injection/production wells in the Eagle Ford Shale, Texas, prior to the MW4.8 20 October 2011 earthquake. *Earth and Planetary Science Letters*, 379, 53–63. <https://doi.org/10.1016/j.epsl.2013.07.02>
- Frohlich, C., Ellsworth, W., Brown, W. A., Brunt, M., Luetgert, J., MacDonald, T., & Walter, S. (2014). The 17 May 2012 M4.8 earthquake near Timpson, East Texas: An event possibly triggered by fluid injection. *Journal of Geophysical Research: Solid Earth*, 119, 581–593. <https://doi.org/10.1002/2013JB010755>
- Galis, M., Ampuero, J. P., Mai, P. M., & Cappa, F. (2017). Induced seismicity provides insight into why earthquake ruptures stop. *Science Advances*, 3(12). <https://doi.org/10.1126/sciadv.aap7528>
- Gan, W., & Frohlich, C. (2013). Gas injection may have triggered earthquakes in the Cogdell oil field, Texas. *Proceedings of the National Academy of Sciences of the United States of America*, 110(47), 18786–18791. <https://doi.org/10.1073/pnas.1311316110>
- Garapati, N., Randolph, J. B., & Saar, M. O. (2015). Brine displacement by CO₂ energy extraction rates, and lifespan of a CO₂-limited CO₂ plume geothermal (CPG) system with a horizontal production well. *Geothermics*, 55, 182–194. <https://doi.org/10.1016/j.geothermics.2015.02.005>
- Ge, S., & Garven, G. (1992). Hydromechanical modeling of tectonically-driven groundwater flow with application to the Arkoma Foreland Basin. *Journal of Geophysical Research*, 97(B6), 9119–1944. <https://doi.org/10.1029/92JB00677>
- Ge, S., Liu, M., Lu, N., Godt, J., & Luo, G. (2009). Did the Zipingpu Reservoir trigger the 2008 Wenchuan earthquake? *Geophysical Research Letters*, 36. <https://doi.org/10.1029/2009GL040349>
- Ghofrani, H., Atkinson, G. M., Schultz, R., & Assatourians, K. (2019). Short-term hindcasts of seismic hazard in the western Canada sedimentary basin caused by induced and natural earthquakes. *Seismological Research Letters*, 90(3). <https://doi.org/10.1785/S0220180285>
- Gischig, V. S., Giardini, D., Amann, F., Hertrich, M., Krietsch, H., Loew, S., et al. (2020). Hydraulic stimulation and fluid circulation experiments in underground laboratories: Stepping up the scale towards engineered geothermal systems. *Geomechanics for Energy and the Environment*, 24, 100175. <https://doi.org/10.1016/j.gete.2019.100175>
- Goebel, T. H. W., Hosseini, S. M., Cappa, F., Hauksson, E., Ampuero, J. P., Aminzadeh, F., & Saleeby, J. B. (2016). Wastewater disposal and earthquake swarm activity at the southern end of the Central Valley, California. *Geophysical Research Letters*, 43, 1092–1099. <https://doi.org/10.1002/2015GL066948>
- Goebel, T. H. W., Weingarten, M., Chen, X., Haffener, J., & Brodsky, E. E. (2017). The 2016 Mw5.1 Fairview, Oklahoma earthquakes: Evidence for long-range poroelastic triggering at >40 km from fluid disposal wells. *Earth and Planetary Science Letters*, 472, 50–61. <https://doi.org/10.1016/j.epsl.2017.05.011>
- Goertz-Allmann, B. P., Kühn, D., Oye, V., Bohloli, B., & Aker, E. (2014). Combining micro-seismic and geomechanical observations to interpret storage integrity at the InSalah CCS site. *Geophysical Journal International*, 198, 447–461. <https://doi.org/10.1093/gji/ggu010>
- Gough, D., & Gough, W. (1970). Load-induced earthquakes at lake Kariba—II. *Geophysical Journal International*, 21(1), 79–101. <https://doi.org/10.1111/j.1365-246X.1970.tb01768.x>
- Grigoli, F., Cesca, S., Priolo, E., Rinaldi, A. P., Clinton, J. F., Stabile, T. A., et al. (2017). Current challenges in monitoring, discrimination, and management of induced seismicity related to underground industrial activities: A European perspective. *Review of Geophysics*, 55, 310–340. <https://doi.org/10.1002/2016RG000542>
- Grigoli, F., Cesca, S., Rinaldi, A. P., Manconi, A., López-Comino, J. A., Clinton, J. F., et al. (2018). The November 2017 Mw 5.5 Pohang earthquake: A possible case of induced seismicity in South Korea. *Science*, 360(6392), 1003–1006. <https://doi.org/10.1126/science.aat2010>
- Guglielmi, Y., Cappa, F., Avouac, J. P., Henry, P., & Elsworth, D. (2015). Induced seismicity. Seismicity triggered by fluid injection-induced aseismic slip. *Science*, 348(6240), 1224–1226. <https://doi.org/10.1126/science.aab0476>
- Gupta, H. K. (2002). A review of recent studies of triggered earthquakes by artificial water reservoirs with special emphasis on earthquakes in Koyana, India. *Earth-Science Reviews*, 58, 279–310. [https://doi.org/10.1016/S0012-8252\(02\)00063-6](https://doi.org/10.1016/S0012-8252(02)00063-6)
- Gupta, H. K., & Chadha, R. (1995). Induced seismicity. *Pure and Applied Geophysics*, 145, 217. Retrieved from https://www.asiaoceania.org/aogs2009/doc/election/Resume_HarshGUPTA.pdf
- Gutenberg, B., & Richter, C. F. (1944). Frequency of earthquakes in California. *Bulletin of the Seismological Society of America*, 36, 185–188. <https://doi.org/10.1785/BSSA0340040185>
- GWPC. (2019). *Produced water report: Regulations, current practices, and research needs* (p. 318). Ground Water Protection Council. Retrieved from https://www.gwpc.org/sites/gwpc/uploads/documents/Research/Produced_Water_Full_Report_Digital_Use.pdf
- Halland, E. K., Riis, F., Magnus, C., Johansen, W. T., Tappel, I. M., Gjeldvik, I. T., et al. (2013). CO₂ storage Atlas of the Norwegian part of the north Sea. *Energy Procedia*, 37, 4919–4926. <https://doi.org/10.1016/j.egypro.2013.06.403>
- Harbaugh, A. W., Banta, E. R., Hill, M. C., & McDonald, M. G. (2000). *MODFLOW-2000, the U.S. Geological Survey modular ground-water model—User guide to modularization concepts and the ground-water flow process* (USGS Open File Report 2000-92, pp. 1–121). Retrieved from <https://pubs.er.usgs.gov/publication/ofr200092>
- Häring, M. O., Schanz, U., Ladner, F., & Dyer, B. C. (2008). Characterisation of the Basel 1 enhanced geothermal system. *Geothermics*, 37, 469–495. <https://doi.org/10.1016/j.geothermics.2008.06.002>
- Healy, J. H., Rubey, W. W., Griggs, D. T., & Raleigh, C. B. (1968). The Denver earthquakes. *Science*, 161, 1301–1310. <https://doi.org/10.1126/science.161.3848.1301>
- Heimlich, C., Gourmelen, N., Masson, F., Schmittbuhl, J., Kim, S.-W., & Azzola, J. (2015). Uplift around the geothermal power plant of Landau (Germany) as observed by InSAR monitoring. *Geothermal Energy*, 3(2), 1–12. <https://doi.org/10.1186/s40517-014-0024-y>
- Hornbach, M. J., DeShon, H. R., Ellsworth, W. L., Stump, B. W., Hayward, C., Frohlich, C., et al. (2015). Causal factors for seismicity near Azle, Texas. *Nature Communications*, 6, 6728. <https://doi.org/10.1038/ncomms7728>
- Hsieh, P. A., & Bredehoeft, J. D. (1981). A reservoir analysis of the Denver earthquakes: A case of induced seismicity. *Journal of Geophysical Research: Solid Earth*, 86, 903–920. <https://doi.org/10.1029/JB086iB02p00903>
- Hubbert, M. K., & Rubey, W. W. (1959). Role of fluid pressure in mechanics of overthrust faulting I. Mechanics of fluid-filled porous solids and its application to overthrust faulting. *The Geological Society of America Bulletin*, 70(2), 115–166. [https://doi.org/10.1130/0016-7606\(1959\)70\[115:ROFPPM\]2.0.CO;2](https://doi.org/10.1130/0016-7606(1959)70[115:ROFPPM]2.0.CO;2)
- Hubbert, M. K., & Willis, D. G. (1957). Mechanics of hydraulic fracturing. *Petroleum Transactions, AIME*, 210, 153–168. <https://doi.org/10.2118/686-G>

- Hui, G., Chen, S., Gu, F., Pang, Y., Yu, X., & Zhang, L. (2021). Insights on controlling factors of hydraulically induced seismicity in the Duvernay East Shale Basin. *Geochemistry, Geophysics, Geosystems*, 22. <https://doi.org/10.1029/2020GC009563>
- Induced seismicity. (2021). Retrieved from <http://inducedearthquakes.org/>
- Ingebritsen, S. E., & Sanford, W. E. (1999). *Groundwater in geologic processes* (p. 341). Cambridge University Press. Retrieved from <https://pubs.er.usgs.gov/publication/70178403>
- Ito, T., & Zoback, M. D. (2000). Fracture permeability and in situ stress to 7 km depth in the KTB Scientific Drillhole. *Geophysical Research Letters*, 27(7), 1045–1048. <https://doi.org/10.1029/1999G1011068>
- Jaeger, J., Cook, N. G., & Zimmerman, R. (2007). *Fundamentals of rock mechanics* (4th ed.). Wiley-Blackwell.
- Jenkins, C. R., Cook, P. J., Ennis-King, J., Undershultz, J., Boreham, C., Dance, T., et al. (2012). Safe storage and effective monitoring of CO₂ in depleted gas fields. *Proceedings of the National Academy of Sciences of the United States of America*, 109(2), E35–E41. <https://doi.org/10.1073/pnas.1107255108>
- Jiang, G., Qiao, X., Wang, X., Lu, R., Liu, L., Yang, H., et al. (2020). GPS observed horizontal ground extension at the Hutubi (China) underground gas storage facility and its application to geomechanical modeling for induced seismicity. *Earth and Planetary Science Letters*, 530, 115943. <https://doi.org/10.1016/j.epsl.2019.115943>
- Jin, L., & Zoback, M. D. (2017). Fully coupled nonlinear fluid flow and poroelasticity in arbitrarily fractured porous media: A hybrid-dimensional computational model. *Journal of Geophysical Research*, 122, 7626–7658. <https://doi.org/10.1002/2017JB014892>
- Johann, L., Dinske, C., & Shapiro, S. A. (2016). Scaling of seismicity induced by nonlinear fluid-rock interaction after an injection stop. *Journal of Geophysical Research*, 121, 8154–8174. <https://doi.org/10.1002/2016JB012949>
- Johann, L., Shapiro, S. A., & Dinske, C. (2018). The surge of earthquakes in Central Oklahoma has features of reservoir-induced seismicity. *Scientific Reports*, 8, 11505. <https://doi.org/10.1038/s41598-018-29883-9>
- Kaven, J. O., Hickman, S. H., McGarr, A. F., & Ellsworth, W. L. (2015). Surface monitoring of microseismicity at the Decatur, Illinois, CO₂ sequestration demonstration site. *Seismological Research Letters*, 86, 1096–1101. <https://doi.org/10.1785/0220150062>
- Kazemi, H. (1969). Pressure transient analysis of naturally fractured reservoirs with uniform fracture distribution. *Society of Petroleum Engineers Journal*, 9(9), 451–462. <https://doi.org/10.2118/2156-A>
- Keränen, K. M., Savage, H. M., Abers, G. A., & Cochran, E. S. (2013). Potentially induced earthquakes in Oklahoma, USA: Links between wastewater injection and the 2011 Mw 5.7 earthquake sequence. *Geology*. <https://doi.org/10.1130/G34045.1>
- Keränen, K. M., & Weingarten, M. (2018). Induced seismicity. *Annual Review of Earth and Planetary Sciences*, 46, 149–174. <https://doi.org/10.1146/annurev-earth-082517-010054>
- Keränen, K., Weingarten, M., Abers, G. A., Bekins, B., & Ge, S. (2014). Sharp increase since 2008 induced by massive wastewater injection. *Science*, 345(6195), 448–451. <https://doi.org/10.1126/science.1255802>
- Kim, K. H., Ree, J. H., Kim, Y., Kim, S., Kang, S. Y., & Seo, W. (2018). Assessing whether the 2017 Mw 5.4 Pohang earthquake in South Korea was an induced event. *Science*, 360(6392), 1007–1009. <https://doi.org/10.1126/science.aat6081>
- Kim, W.-Y. (2013). Induced seismicity associated with fluid injection into a deep well in Youngstown, Ohio. *Journal of Geophysical Research*, 118, 3506–3518. <https://doi.org/10.1002/jgrb.50247>
- King, F. H. (1892). *Observations and experiments on the fluctuations in the level and rate of movement of ground water on the Wisconsin Agricultural Experiment Station Farm, and at Whitewater, Wisconsin* (Vol. 5, pp. 67–69). U.S. Weather Bureau Bulletin.
- King, G. C. P., Stein, R. S., & Lin, J. (1994). Static stress changes and the triggering of earthquakes. *Bulletin of the Seismological Society of America*, 84(3), 935–953. <https://doi.org/10.1785/BSSA0840030935>
- Kong, X.-Z., & Saar, M. O. (2013). Numerical study of the effects of permeability heterogeneity on density-driven convective mixing during CO₂ dissolution storage. *International Journal of Greenhouse Gas Control*, 19, 160–173. <https://doi.org/10.1016/j.ijggc.2013.08.020>
- Kranz, R. L., Saltzman, J. S., & Blacic, J. D. (1990). Hydraulic diffusivity measurements on laboratory rock samples using an oscillating pore pressure method. *International Journal of Rock Mechanics and Mining Science & Geomechanics Abstracts*, 27(5), 345–352. [https://doi.org/10.1016/0148-9062\(90\)92709-N](https://doi.org/10.1016/0148-9062(90)92709-N)
- Leal, A. M. M., Kulik, D. A., Smith, W. R., & Saar, M. O. (2017). An overview of computational methods for chemical equilibrium and kinetic calculations for geochemical and reactive transport modeling. *Pure and Applied Chemistry*, 89(5), 597–643. <https://doi.org/10.1515/pac-2016-1107>
- Lei, X., Ma, S., Chen, W., Pang, C., Zeng, J., & Jiang, B. (2013). A detailed view of the injection-induced seismicity in a natural gas reservoir in Zigong, southwestern Sichuan Basin, China. *Journal of Geophysical Research*, 118(8), 4296–4311. <https://doi.org/10.1002/jgrb.50310>
- Leonard, M. (2010). Earthquake fault scaling: Self-consistent relating of rupture length, width, average displacement, and moment release. *Bulletin of the Seismological Society of America*, 100(5A), 1971–1988. <https://doi.org/10.1785/0120090189>
- Lin, J., & Stein, R. S. (2004). Stress triggering in thrust and subduction earthquakes and stress interaction between the southern San Andreas and nearby thrust and strike-slip faults. *Journal of Geophysical Research*, 109, B02303. <https://doi.org/10.1029/2003JB002607>
- Lindeberg, E., Vuillaume, J.-F., & Ghaderi, A. (2009). Determination of the CO₂ storage capacity of the Utsira formation. *Energy Procedia*, 1, 2777–2784. <https://doi.org/10.1016/J.EGYPRO.2009.02.049>
- Lockner, D., & Byerlee, J. D. (1977). Hydrofracture in Weber sandstone at high confining pressure and differential stress. *Journal of Geophysical Research*, 82(14), 2018–2026. <https://doi.org/10.1029/JB082I014P02018>
- Luhmann, A. J., Kong, X.-Z., Tutolo, B. M., Ding, K., Saar, M. O., & Seyfried, W. E., Jr. (2013). Permeability reduction produced by grain reorganization and accumulation of exsolved CO₂ during geologic carbon sequestration: A new CO₂ trapping mechanism. *Environmental Science and Technology*, 47, 242–251. <https://doi.org/10.1021/es3031209>
- Luhmann, A. J., Kong, X.-Z., Tutolo, B. M., Garapati, N., Bagley, B. C., Saar, M. O., & Seyfried, W. E., Jr. (2014). Experimental dissolution of dolomite by CO₂-charged brine at 100°C and 150 bar: Evolution of porosity, permeability, and reactive surface area. *Chemical Geology*, 380:145–160. <https://doi.org/10.1016/j.chemgeo.2014.05.001>
- Luhmann, A. J., Tutolo, B. M., Bagley, B. C., Mildner, D. F. R., Seyfried, W. E., Jr., & Saar, M. O. (2017). Permeability, porosity, and mineral surface area changes in basalt cores induced by reactive transport of CO₂-rich brine. *Water Resources Research*, 53, 1908–1927. <https://doi.org/10.1002/2016WR019216>
- Ma, J., Querci, L., Hattendorf, B., Saar, M. O., & Kong, X.-Z. (2020). The effect of mineral dissolution on the effective stress law for permeability in a tight sandstone. *Geophysical Research Letters*, 47, e2020GL088346. <https://doi.org/10.1029/2020GL088346>
- Mahani, A. B., Schultz, R., Kao, H., Walker, D., Johnson, J., & Salas, C. (2017). Fluid injection and seismic activity in the northern Montney Play, British Columbia, Canada, with special reference to the 17 August 2015 Mw 4.6 induced earthquake. *Bulletin of the Seismological Society of America*, 107, 542–552. <https://doi.org/10.1785/0120160175>
- Majer, E. L., Baria, R., Stark, M., Oates, S., Bommer, J., Smith, B., & Asanuma, H. (2007). Induced seismicity associated with enhanced geothermal systems. *Geothermics*, 36, 185–222. <https://doi.org/10.1016/j.geothermics.2007.03.003>

- Mandl, G. (1988). *Mechanics of tectonic faulting* (p. 407). Elsevier.
- McGarr, A. (2014). Maximum magnitude earthquakes induced by fluid injection. *Journal of Geophysical Research*, *119*, 1008–1019. <https://doi.org/10.1002/2013jb010597>
- McGarr, A., & Barbour, A. J. (2017). Wastewater disposal and the earthquake sequences during 2016 near Fairview, Pawnee, and Cushing, Oklahoma. *Geophysical Research Letters*, *44*, 9330–9336. <https://doi.org/10.1002/2017GL075258>
- McGarr, A., Simpson, D., & Seeber, L. (2002). Case histories of induced and triggered seismicity. In W. Lee, H. Kanamori, P. Jennings, & C. Kisslinger, (Eds.), *International handbook of earthquake and engineering seismology* (Chap. 40, v81A, 647–661). Elsevier.
- Meremonte, M. E., Lahr, J. C., Frankel, A. D., Dewey, J. W., Crone, A. J., Overturf, D. E., et al. (2002). *Investigation of an earthquake swarm near Trinidad, Colorado*. (open-file report 02-0073). US Geological Survey.
- Moench, A. F. (1984). Double-porosity models for fissured groundwater reservoir with fracture skin. *Water Resources Research*, *20*(7), 831–846. <https://doi.org/10.1029/WR020i007p00831>
- Molina, I., Velásquez, J. S., Rubinstein, J. L., Garcia-Aristizabal, A., & Dionicio, V. (2020). Seismicity induced by massive wastewater injection near Puerto Gaitán, Colombia. *Geophysical Journal International*, *223*, 777–791. <https://doi.org/10.1093/gji/ggaa326>
- Mossop, A., & Segall, P. (1997). Subsidence at the Geysers geothermal field, N. California from a comparison of GPS and leveling surveys. *Geophysical Research Letters*, *24*(14), 1839–1842. <https://doi.org/10.1029/97GL51792>
- Mukuhira, Y., Dinske, C., Asanuma, H., Ito, T., & Häring, M. O. (2017). Pore pressure behavior at the shut-in phase and causality of large induced seismicity at Basel, Switzerland. *Journal of Geophysical Research*, *122*, 411–435. <https://doi.org/10.1002/2016JB013338>
- Nakai, J. S., Weingarten, M., Sheehan, A. F., Bilek, S. L., & Ge, S. (2017). A possible causative mechanism of Raton Basin, New Mexico and Colorado earthquakes using recent seismicity patterns and pore pressure modeling. *Journal of Geophysical Research*, *122*. <https://doi.org/10.1002/2017JB014415c>
- Nelson, P. H., Gianoutsos, N. J., & Drake, D. M. (2015). Underpressure in Mesozoic and Paleozoic rock units in the Midcontinent of the United States. *AAPG Bulletin*, *99*, 1861–1892. <https://doi.org/10.1306/04171514169>
- Nicholson, C., & Wesson, R. L. (1992). Triggered earthquakes and deep well activities. *Pure and Applied Geophysics*, *139*, 561–578. <https://doi.org/10.1007/BF00879951>
- O'Brien, S. O., Hallaway, A., & Bacci, V. O. (2018, October 21–26). *Quest CCS facility: Microseismic observations*. Paper presented at the 14th International Conference on Greenhouse Gas Control Technologies (GHGT-14). Retrieved from https://papers.ssrn.com/sol3/papers.cfm?abstract_id=3366114
- Ogware, P. O., DeShon, H. R., & Hornbach, M. J. (2018). The Dallas-Fort Worth Airport earthquake sequence: Seismicity beyond injection period. *Journal of Geophysical Research*, *123*, 553–563. <https://doi.org/10.1002/2017JB015003>
- Okada, Y. (1992). Internal deformation due to shear and tensile faults in a half-space. *Bulletin of the Seismological Society of America*, *82*(2), 1018–1040. <https://doi.org/10.1785/BSSA0820021018>
- Onuma, T., & Ohkawa, S. (2009). Detection of surface deformation related with CO₂ injection by DInSAR at in Salah, Algeria. *Energy Procedia*, *1*, 2177–2184. <https://doi.org/10.1016/j.egypro.2009.01.283>
- Paulding, B. W., Jr. (1967). *Orientation of hydraulically induced fractures* (ARMA 67-0461, pp. 461–489). American Rock Mechanics Association.
- Peterie, S. L., Miller, R. D., Intfen, J. W., & Gonzales, J. B. (2018). Earthquakes in Kansas induced by extremely far-field pressure diffusion. *Geophysical Research Letters*, *45*(1), 395–401. <https://doi.org/10.1002/2017GL076334>
- Petersen, M. D., Mueller, C. S., Moschetti, M. P., Hoover, S. M., Llenos, A. L., Ellsworth, W. L., et al. (2016). Seismic-hazard forecast for 2016 including induced and natural earthquakes in the central and eastern United States. *Seismological Research Letters*, *87*(6), 1327–1341. <https://doi.org/10.1785/0220160072>
- Petersen, M. D., Mueller, C. S., Moschetti, M. P., Hoover, S. M., Rukstales, K. S., McNamara, D. E., et al. (2018). 2018 one-year seismic hazard forecast for the central and eastern United States from induced and natural earthquakes. *Seismological Research Letters*, *89*(3), 1049–1061. <https://doi.org/10.1785/0220180005>
- Pollyea, R. M., Chapman, M. C., Jayne, R. S., & Wu, H. (2019). High density oilfield wastewater disposal causes deeper, stronger, and more persistent earthquakes. *Nature Communications*, *10*. <https://doi.org/10.1038/s41467-019-11029-8>
- Pollyea, R. M., Mohammadi, N., Taylor, J. E., & Chapman, M. C. (2018). Geospatial analysis of Oklahoma (USA) earthquakes (2011–2016): Quantifying the limits of regional-scale earthquake mitigation measures. *Geology*, *46*, 215–218. <https://doi.org/10.1130/G39945.1>
- Prinet, C., Thibeau, S., Lescanne, M., & Monne, J. (2013). Lacq-Rousse CO₂ capture and storage demonstration pilot: Lessons learnt from two and a half years monitoring. *Energy Procedia*, *37*, 3610–3620. <https://doi.org/10.1016/j.egypro.2013.06.254>
- Raleigh, C. B., Healy, J. H., & Bredehoeft, J. D. (1976). An experiment in earthquake control at Rangely, Colorado. *Science*, *191*, 1230–1237. doi: 10.1126/science.1230123
- Rice, J. R., & Cleary, M. (1976). Some basic stress diffusion solutions for fluid-saturated elastic porous media with compressible constituents. *Reviews of Geophysics*, *14*, 227–241. doi: 10.1029/1976RG000141
- Riffault, J., Dempsey, D., Karra, S., & Archer, R. (2018). Microseismicity cloud can be substantially larger than the associated stimulated fracture volume: The case of the Parana enhanced geothermal system. *Journal of Geophysical Research*, *123*(8), 6845–6870. <https://doi.org/10.1029/2017JB015299>
- Ringrose, P. S., Mathieson, A. S., Wright, I. W., Selama, F., Hansen, O., Bissell, R., et al. (2013). The in Salah CO₂ storage project: Lessons learned and knowledge transfer. *Energy Procedia*, *37*, 6226–6236. <https://doi.org/10.1016/j.egypro.2013.06.551>
- Roeloffs, E. A. (1988). Fault stability changes induced beneath a reservoir with cyclic variation in water level. *Journal of Geophysical Research*, *93*(B3), 2107–2124. <https://doi.org/10.1029/JB093iB03p02107>
- Rothert, E., & Shapiro, S. A. (2003). Microseismic monitoring of borehole fluid injections: Data modeling and inversion for hydraulic properties of rocks. *Geophysics*, *68*, 685–689. <https://doi.org/10.1190/1.1567239>
- Rubinstein, J. L., Barbour, A. J., & Norbeck, J. H. (2021). Forecasting induced earthquake hazard using a hydromechanical earthquake nucleation model. *Seismological Research Letters*, *92*, 2206–2220. <https://doi.org/10.1785/0220200215>
- Rubinstein, J. L., Ellsworth, W. L., McGarr, A., & Benz, H. M. (2014). The 2001–present induced earthquake sequence in the Raton Basin of northern New Mexico and southern Colorado. *Bulletin of the Seismological Society of America*, *104*(5), 2162–2181. <https://doi.org/10.1785/0120140009>
- Rudnicki, J. W. (1986). Fluid mass sources and point forces in linear elastic diffusive solids. *Mechanics of Materials*, *5*(4), 383–393. [https://doi.org/10.1016/0167-6636\(86\)90042-6](https://doi.org/10.1016/0167-6636(86)90042-6)
- Saar, M. O., & Manga, M. (2003). Seismicity induced by seasonal groundwater recharge at Mt. Hood, Oregon. *Earth and Planetary Science Letters*, *214*, 605–618. [https://doi.org/10.1016/S0012-821X\(03\)00418-7](https://doi.org/10.1016/S0012-821X(03)00418-7)
- Sáez, A., Lecampion, B., Bhattacharya, P., & Viesca, R. C. (2021). *Three-dimensional aseismic ruptures driven by fluid injection* (EGU21-13394). EGU General Assembly. Retrieved from <https://meetingorganizer.copernicus.org/EGU21/EGU21-13394.html>

- Schultz, R., Skoumal, R. J., Brudzinski, M. R., Eaton, D., Baptie, B., & Ellsworth, W. (2020). Hydraulic fracturing-induced seismicity. *Reviews of Geophysics*, 58, e2019RG000695. <https://doi.org/10.1029/2019RG000695>
- Schultz, R., Stern, V., Novakovic, M., Atkinson, G., & Gu, Y. (2015). Hydraulic fracturing and the Crooked Lake Sequences: Insights gleaned from regional seismic networks. *Geophysical Research Letters*, 42, 2750–2758. <https://doi.org/10.1002/2015GL063455>
- Schultz, R., Wang, R., Gu, Y. J., Haug, K., & Atkinson, G. (2017). A seismological overview of the induced earthquakes in the Duvernay play near Fox Creek, Alberta. *Journal of Geophysical Research*, 122, 492–505. <https://doi.org/10.1002/2016JB013570>
- Scuderi, M. M., Tinti, E., Cocco, M., & Collettini, C. (2020). The role of shear fabric in controlling breakdown processes during laboratory slow-slip events. *Journal of Geophysical Research: Solid Earth*, 125, e2020JB020405. <https://doi.org/10.1029/2020JB020405>
- Segall, P. (1985). Stress and subsidence resulting from subsurface fluid withdrawal in the epicentral region of the 1983 Coalinga earthquake. *Journal of Geophysical Research*, 90(B8), 6801–6816. <https://doi.org/10.1029/JB090iB08p06801>
- Segall, P. (1989). Earthquakes triggered by fluid extraction. *Geology*, 17, 942–946. [https://doi.org/10.1130/0091-7613\(1989\)017<0942:ETBFE>2.3.CO;2](https://doi.org/10.1130/0091-7613(1989)017<0942:ETBFE>2.3.CO;2)
- Segall, P. (2010). *Earthquake and volcano deformation* (p. 432). Princeton University Press.
- Segall, P., Grasso, J. R., & Mossop, A. (1994). Poroelastic stressing and induced seismicity near the Lacq Gas Field, Southwestern France. *Journal of Geophysical Research*, 99(B8), 15423–15438. <https://doi.org/10.1029/94JB00989>
- Segall, P., & Lu, S. (2015). Injection-induced seismicity: Poroelastic and earthquake nucleation effects. *Journal of Geophysical Research*, 120, 5082–5103. <https://doi.org/10.1002/2015JB012060>
- Shapiro, S. A., & Dinske, C. (2009). Scaling of seismicity induced by nonlinear fluid-rock interaction. *Journal of Geophysical Research*, 114, B09307. <https://doi.org/10.1029/2008JB006145>
- Shapiro, S. A., Huenges, E., & Borm, G. (1997). Estimating the crust permeability from fluid-injection-induced seismic emission at the KTB site. *Geophysical Journal International*, 131, F15–F18. <https://doi.org/10.1111/j.1365-246X.1997.tb01215.x>
- Shapiro, S. A., Krüger, O. S., Dinske, C., & Langenbruch, C. (2011). Magnitudes of induced earthquakes and geometric scales of fluid-stimulated rock volumes. *Geophysics*, 76(6), WC55–WC63. <https://doi.org/10.1190/geo2010-0349.1>
- Shapiro, S. A., Rotherth, E., Rathz, V., & Rindschwentner, J. (2002). Characterization of fluid transport properties of reservoirs using induced microseismicity. *Geophysics*, 67(1), 212–220. <https://doi.org/10.1190/1.1451597>
- Shen, L. W., Schmitt, D. R., & Schultz, R. (2019). Frictional stabilities on induced earthquake fault planes at Fox Creek, Alberta: A pore fluid pressure dilemma. *Geophysical Research Letters*, 46, 8753–8762. <https://doi.org/10.1029/2019GL083566>
- Shen, L. W., Schmitt, D. R., Wang, R., & Hauck, T. E. (2021). States of in situ stress in the Duvernay East Shale Basin and Willesden Green of Alberta, Canada: Variable in situ stress states effect fault stability. *Journal of Geophysical Research*, 126. <https://doi.org/10.1029/2020JB021221>
- Shirzaei, M., Ellsworth, W., Tiampo, K., Gonzalez, P. J., & Manga, M. (2016). Surface uplift and time-dependent seismic hazard due to fluid injection in eastern Texas. *Science*, 353, 1416–1419. <https://doi.org/10.1126/science.aag0262>
- Shirzaei, M., Manga, M., & Zhai, G. (2019). Hydraulic properties of injection formations constrained by surface deformation. *Earth and Planetary Science Letters*, 515, 125–134. <https://doi.org/10.1016/j.epsl.2019.03.025>
- Simpson, D. W., Leith, W. S., & Scholz, C. H. (1988). Two types of reservoir-induced seismicity. *Bulletin of the Seismological Society of America*, 78, 2025–2040. <https://doi.org/10.1785/BSSA0780062025>
- Skoumal, R. J., Brudzinski, M. R., & Currie, B. S. (2015). Induced earthquakes during hydraulic fracturing in Poland Township, Ohio. *Bulletin of the Seismological Society of America*, 105(1), 189–197. <https://doi.org/10.1785/0120140168>
- Snee, J. L., & Zoback, M. D. (2018). *State of stress in the Permian Basin, Texas and New Mexico: Implications for induced seismicity*. The Leading Edge. <https://doi.org/10.1190/tle37020127.1>
- Solberg, P., Lockner, D., & Byerlee, J. (1977). Shear and tension hydraulic fractures in low permeability rocks. *Pure and Applied Geophysics*, 115, 191–198. <https://doi.org/10.1007/BF01637103>
- Stein, R. S. (1999). The role of stress transfer in earthquake occurrence. *Nature*, 402, 605–609. <https://doi.org/10.1038/45144>
- Stein, R. S. (2005). Earthquake conversations. *Scientific American*, 15(2), 82–89. <https://doi.org/10.1038/scientificamerican0705-82sp>
- Stork, A. L., Nixon, C. G., Hawkes, C. D., Birnie, C., White, D. J., Schmitt, D. R., & Roberts, B. (2018). Is CO₂ injection at Aquistore aseismic? A combined seismological and geomechanical study of early injection operations. *International Journal of Greenhouse Gas Control*, 75, 107–124. <https://doi.org/10.1016/j.ijggc.2018.05.016>
- Stork, A. L., Verdon, J. P., & Kendall, J.-M. (2015). The microseismic response at the in Salah carbon capture and storage (CCS) site. *International Journal of Greenhouse Gas Control*, 32, 159–171. <https://doi.org/10.1016/j.ijggc.2014.11.014>
- Suckale, J. (2009). Induced seismicity in hydrocarbon fields. *Advances in Geophysics*, 51, 55–106. [https://doi.org/10.1016/S0065-2687\(09\)05107-3](https://doi.org/10.1016/S0065-2687(09)05107-3)
- Sumy, D. F., Cochran, E. S., Keranen, K. M., Wei, M., & Abers, G. A. (2014). Observations of static Coulomb stress triggering of the November 2011 M5.7 Oklahoma earthquake sequence. *Journal of Geophysical Research*, 119, 1904–1923. <https://doi.org/10.1002/2013JB010612>
- Talwani, P. (1997). On the nature of reservoir-induced seismicity. *Pure and Applied Geophysics*, 150, 473–492. https://doi.org/10.1007/978-3-0348-8814-1_8
- Terzaghi, K. (1936). The shearing resistance of saturated soils. *International Society for Soil Mechanics and Geotechnical Engineering*, 1, 54–56. Retrieved from https://www.issmge.org/uploads/publications/1/44/1936_01_0017.pdf
- Theis, C. V. (1935). The relation between the lowering of the piezometric surface and the rate and duration of discharge of a well using ground water storage. *Eos Transactions American Geophysical Union*, 16(2), 519–524. <https://doi.org/10.1029/TR016i002p00519>
- Toda, S., Lin, J., & Stein, R. S. (2011). Using the 2011 Mw 9.0 off the Pacific coast of Tohoku earthquake to test the Coulomb stress triggering hypothesis and to calculate faults brought closer to failure. *Earth Planets and Space*, 63(7), 725–730. <https://doi.org/10.5047/eps.2011.05.010>
- Toda, S., Stein, R. S., Beroza, G. C., & Marsan, D. (2012). Aftershocks halted by static stress shadows. *Nature Geoscience*, 5(6), 410–413. <https://doi.org/10.1038/ngeo1465>
- Toda, S., Stein, R. S., Richards-Dinger, K. B., & Bozkurt, S. B. (2005). Forecasting the evolution of seismicity in southern California: Animations built on earthquake stress transfer. *Journal of Geophysical Research*, 110, B05S16. <https://doi.org/10.1029/2004JB003415>
- Townend, J., & Zoback, M. D. (2000). How faulting keeps the crust strong. *Geology*, 28(5), 399–402. [https://doi.org/10.1130/0091-7613\(2000\)28<399:HFKTCS>2.0.CO;2](https://doi.org/10.1130/0091-7613(2000)28<399:HFKTCS>2.0.CO;2)
- Tung, S., Zhai, G., & Shirzaei, M. (2021). Potential link between 2020 Mentone, West Texas M5 earthquake and nearby wastewater injection: Implications for aquifer mechanical properties. *Geophysical Research Letters*, 48, e2020GL090551. <https://doi.org/10.1029/2020GL090551>
- Tutolo, B. M., Kong, X.-Z., Seyfried, W. E., Jr., & Saar, M. O. (2015). High performance reactive transport simulations examining the effects of thermal, hydraulic, and chemical (THC) gradients on fluid injectivity at carbonate CCUS reservoir scales. *International Journal of Greenhouse Gas Control*, 39, 285–301. <https://doi.org/10.1016/j.ijggc.2015.05.026>
- Tutolo, B. M., Luhmann, A. J., Kong, X.-Z., Bagley, B., Alba-Venero, D., Mitchell, N., et al. (2020). Contributions of visible and invisible pores to reactive transport in dolomite. *Geochemical Perspectives Letters*, 14, 42–46. <https://doi.org/10.7185/geochemlet.2022>

- Tutolo, B. M., Luhmann, A. J., Kong, X.-Z., Saar, M. O., & Seyfried, W. E., Jr. (2014). Experimental observation of permeability changes in dolomite at CO₂ sequestration conditions. *Environmental Science and Technology*, 8, 2445–2452. <https://doi.org/10.1021/es4036946>
- van der Elst, N. J., Page, M. T., Weiser, D. A., Goebel, T. H. W., & Hosseini, S. M. (2016). Induced earthquake magnitudes are as large as (statistically) expected. *Journal of Geophysical Research*, 121, 4575–4590. <https://doi.org/10.1002/2016JB012818>
- Vasco, D. W., Rucci, A., Ferretti, A., Novali, F., Bissell, R. C., Ringrose, P. S., et al. (2010). Satellite-based measurements of surface deformation reveal fluid flow associated with the geological storage of carbon dioxide. *Geophysical Research Letters*, 37, L03303. <https://doi.org/10.1029/2009GL041544>
- Verdon, J. P., Kendall, J.-M., Stork, A. L., Chadwick, R. A., White, D. J., & Bissell, R. C. (2013). Comparison of geomechanical deformation induced by megaton-scale CO₂ storage at Sleipner, Weyburn, and in Salah. *Proceedings of the National Academy of Sciences of the United States of America*, 110, E2762–E2771. <https://doi.org/10.1073/pnas.1302156110>
- Verdon, J. P., Kendall, J.-M., White, D. J., & Angus, D. A. (2011). Linking microseismic event locations with geomechanical models to minimise the risks of storing CO₂ in geological formations. *Earth and Planetary Science Letters*, 305, 143–152. <https://doi.org/10.1016/j.epsl.2011.02.048>
- Verdon, J. P., Stork, A. L., Bissell, R. C., Bond, C. E., & Werner, M. J. (2015). Simulation of seismic events induced by CO₂ injection at in Salah, Algeria. *Earth and Planetary Science Letters*, 426, 118–129. <https://doi.org/10.1016/j.epsl.2015.06.029>
- Verruijt, A. (2014). *Theory and problems in poroelasticity*. Retrieved from <https://vulcanhammer.net/files.wordpress.com/2017/01/poroelasticity2014.pdf>
- Vilarrasa, V., & Carrera, J. (2015). Geologic carbon storage is unlikely to trigger large earthquakes and reactivate faults through which CO₂ could leak. *Proceedings of the National Academy of Sciences of the United States of America*, 112, 5938–5943. <https://doi.org/10.1073/pnas.1413284112>
- Vilarrasa, V., Carrera, J., Olivella, S., Rutqvist, J., & Laloui, L. (2019). Induced seismicity in geologic carbon storage. *Solid Earth*, 10, 871–892. <https://doi.org/10.5194/se-10-871-2019>
- Wang, C.-Y., & Manga, M. (2021). *Water and earthquakes. Lecture notes in earth system Sciences*. Springer.
- Wang, H. (2000). *Theory of linear poroelasticity with applications to geomechanics and hydrogeology*. Princeton University Press.
- Wang, R., & Kumpel, H.-J. (2003). Poroelasticity: Efficient modeling of strongly coupled, slow deformation processes in multilayered half-space. *Geophysics*, 68(2), 1–13. <https://doi.org/10.1190/1.1567241>
- Warren, J. E., & Root, P. J. (1963). The behaviour of naturally fractured reservoirs. *Society of Petroleum Engineers Journal*, 3, 245–255. <https://doi.org/10.2118/426-PA>
- Wei, S., Avouac, J., Hudnut, K. W., Donnellan, A., Parker, J. W., Graves, R. W., et al. (2015). The 2012 Brawley swarm triggered by injection-induced aseismic slip. *Earth and Planetary Science Letters*, 422, 115–125. <https://doi.org/10.1016/j.epsl.2015.03.054>
- Weingarten, M. B. (2015). *On the interaction between fluids and earthquakes in both natural and induced seismicity* (Dissertation), University of Colorado Boulder.
- Weingarten, M. B., Ge, S., Godt, J. W., Bekins, B. A., & Rubinstein, J. L. (2015). High-rate injection is associated with the increase in U.S. mid-continent seismicity. *Science*, 348, 1336–1340. <https://doi.org/10.1126/science.aab1345>
- Wells, D. L., & Coppersmith, K. J. (1994). New empirical relationships among magnitude, rupture length, rupture width, rupture area, and surface displacement. *Bulletin of the Seismological Society of America*, 84(4), 974–1002. <https://doi.org/10.1785/BSSA0840040974>
- Wilson, M. P., Foulger, G. R., Gluyas, J. G., Davies, R. J., & Julian, B. R. (2017). HiQuake: The human-induced earthquake database. *Seismological Research Letters*, 88(6), 1560–1565. <https://doi.org/10.1785/0220170112>
- Yang, F., Babarinde, O. O., Okwen, R., Frailey, S. M., & Whittaker, S. G. (2018). *Modeling commercial-scale CO₂ injection in Mt. Simon sandstone near Decatur, IL storage sites*. Paper presented at the 14th International Conference on Greenhouse Gas Control Technologies (GHGT-14). Social Science Research Network.
- Yeck, W., Hayes, G., McNamara, D., Rubinstein, J., Barnhart, W., Earle, P., & Benz, H. (2017). Oklahoma experiences largest earthquake during ongoing regional wastewater injection hazard mitigation efforts. *Geophysical Research Letters*, 44, 711–717. <https://doi.org/10.1002/2016GL071685>
- Yeo, I. W., Brown, M. R. M., Ge, S., & Lee, K. K. (2020). Causal mechanism of injection-induced earthquakes through the Mw 5.5 Pohang earthquake case study. *Nature Communications*, 11, 2614. <https://doi.org/10.1038/s41467-020-16408-0>
- Zang, A., Oye, V., Jousset, P., Deichmann, N., Gritto, R., McGarr, A., et al. (2014). Analysis of induced seismicity in geothermal reservoirs—An overview. *Geothermics*, 52, 6–21. <https://doi.org/10.1016/j.geothermics.2014.06.005>
- Zhai, G., Shirzaei, M., & Manga, M. (2020). Elevated seismic hazard in Kansas due to high-volume injections in Oklahoma. *Geophysical Research Letters*, 47, e2019GL085705. <https://doi.org/10.1029/2019GL085705>
- Zhai, G., Shirzaei, M., & Manga, M. (2021). Widespread deep seismicity in the Delaware Basin, Texas, is mainly driven by shallow wastewater injection. *Proceedings of the National Academy of Sciences of the United States of America*, 118(20), e2102338118. <https://doi.org/10.1073/pnas.2102338118>
- Zhai, G., Shirzaei, M., Manga, M., & Chen, X. (2019). Pore-pressure diffusion, enhanced by poroelastic stresses, controls induced seismicity in Oklahoma. *Proceedings of the National Academy of Sciences of the United States of America*, 116, 16228–16233. <https://doi.org/10.1073/pnas.1819225116>
- Zhang, M., Ge, S., Yang, Q., & Ma, X. (2021). Impoundment-associated hydro-mechanical changes and regional seismicity near the Xiluodu reservoir, Southwestern China. *Journal of Geophysical Research: Solid Earth*, 126, e2020JB021590. <https://doi.org/10.1029/2020JB021590>
- Zhang, Y., Person, M., Rupp, J., Ellett, K., Celia, M. A., Gable, C. W., et al. (2013). Hydrogeologic controls on induced seismicity in crystalline basement rocks due to fluid injection into basal reservoirs. *Groundwater*, 51(4), 525–538. <https://doi.org/10.1111/gwat.12071>
- Zoback, M., & Gorelick, S. (2012). Earthquake triggering and large-scale geologic storage of carbon dioxide. *Proceedings of the National Academy of Sciences of the United States of America*, 112(33), E4510. <https://doi.org/10.1073/pnas.1508533112>
- Zoback, M., & Gorelick, S. (2015). To prevent earthquake triggering, pressure changes due to CO₂ injection need to be limited. *Proceedings of the National Academy of Sciences of the United States of America*, 109, 10164–10168. doi: